Scholars' Mine

Fall 2012

Meso-scale fluidic devices with chemical sensors for biological applications

Satya Gowthami Achanta

MESO-SCALE FLUIDIC DEVICES WITH CHEMICAL SENSORS FOR

BIOLOGICAL APPLICATIONS

by

SATYA ACHANTA

A DISSERTATION

Presented to the Faculty of the Graduate School of the

MISSOURI UNIVERSITY OF SCIENCE & TECHNOLOGY

In Partial Fulfillment of the Requirements for the Degree

DOCTOR OF PHILOSOPHY

in

CHEMICAL ENGINEERING

2012

Approved by:

Dr. David Westenberg, Advisor
Dr. Chang-Soo Kim
Dr.David Henthorn
Dr. Douglas Ludlow
Dr. Ronald Frank
Dr. Katie Shannon

PUBLICATION DISSERTATION OPTION

This dissertation consists of the following articles that will be submitted for publication as follows:

Pages 15-31 are intended for submission to IEEE SENSORS Journal

Pages 47-64 are intended for submission to LAB-ON-A-CHIP Journal

Pages 67-82 are intended for submission to LAB-ON-A-CHIP Journal

ABSTRACT

Molecular oxygen and humidity are some of the major environmental quantities being measured for various industrial and commercial applications. This dissertation focuses on the design, fabrication and characterization of optofluidic biosensor systems for oxygen and humidity quantification using color charge-coupled device (CCD) camera as a photodetector and LED panel as an excitation source. Meso-scale fluidic devices with integrated oxygen and humidity sensors for potential applications to hydrotropic and oxytropic studies of small plant roots have been investigated in this study. Meso-scale sensor platform was fabricated using porphyrine complex as the sensitive dye embedded within Ethyl Cellulose (EC) polymer matrix. Green LED light displayed from the light panel helped in exciting the oxygen complex by emitting varied fluorescence emission corresponding to oxygen. This method of optical oxygen imaging helps in wide area distribution over the sensor platform.

The root tip response to environmental stimuli by directed growth plays a major role in plant development. With these tropic responses of roots, plants can help themselves during environmental risks such as drought conditions. Different fluidic devices were fabricated with embedded humidity sensors within the device to study the effect of tropic responses. Hydrotropic behavior of corn roots was analyzed along with humidity gradient quantification using color charge-coupled device (CCD) camera for both imaging of the plant root and profiling of humidity distribution. Successfully created and analyzed the humidity gradient which resulted in root orientation because of hydrotropic response indicating the effectiveness of this device for further biological applications.

ACKNOWLEDGEMENTS

TABLE OF CONTENTS

Page

LIST OF ILLUSTRATIONS

PAPER IV

LIST OF TABLES

1. INTRODUCTION

Molecular oxygen and humidity are some of the major environmental quantities being measured for various industrial and commercial applications. Consequently, there are many application fields where the oxygen and humidity determination is critical. This dissertation focuses on the design, fabrication and characterization of optofluidic biosensor systems for oxygen and humidity quantification using color charge-coupled device (CCD) camera as a photodetector and LCD screen as an excitation source. Meso-scale fluidic devices with integrated oxygen and humidity sensors for potential applications to hydrotropic and oxytropic studies of small plant roots have been investigated in this study.

1.1. OXYGEN SENSORS

1.1.1. Electrochemical Methods.
Electrochemical way of oxygen sensing is one of well-developed techniques for several years, which include Galvin type or Clark type oxygen electrodes. A typical Clark's electrode is made up of a cathode, an anode and an electrolyte solution. These electrodes are in common use because of their easy calibration and inexpensive instrumentation. Miniaturized electrodes have been explored with wide variety of applications in medical and clinical monitoring. However, this electrochemical quantification has its own limitations, such as consumption of oxygen during the process of measurement, short lifetime and frequent filling of electrolyte solution, etc.

1.1.2. Optical Methods.
In order to overcome the drawbacks of electrochemical sensors, optical oxygen sensors have emerged as an alternative approach with luminescence quenching as its principle mechanism and oxygen as a powerful quencher

[1-6]. They utilize fluorophores as oxygen sensitive dye molecules which emits
fluorescence when excited at a particular wavelength. Quenching is a phenomenon of
decrease in the emission intensity of a fluorophore when in contact with a quencher,
through a non-radiative transfer of energy to the quencher, as shown in figure 1.1. The
degree of quenching depends on the concentration of oxygen. The basic advantages of
these optical oxygen sensors include their non-consumption of oxygen during sensing,
sensor miniaturization and sensitivity, quick response time, etc.

Excited state

$\lambda_{emission}$

$\lambda_{excitation}$

F

O_2

Excited state

No photon emission because of
non-radiative energy transfer to
oxygen
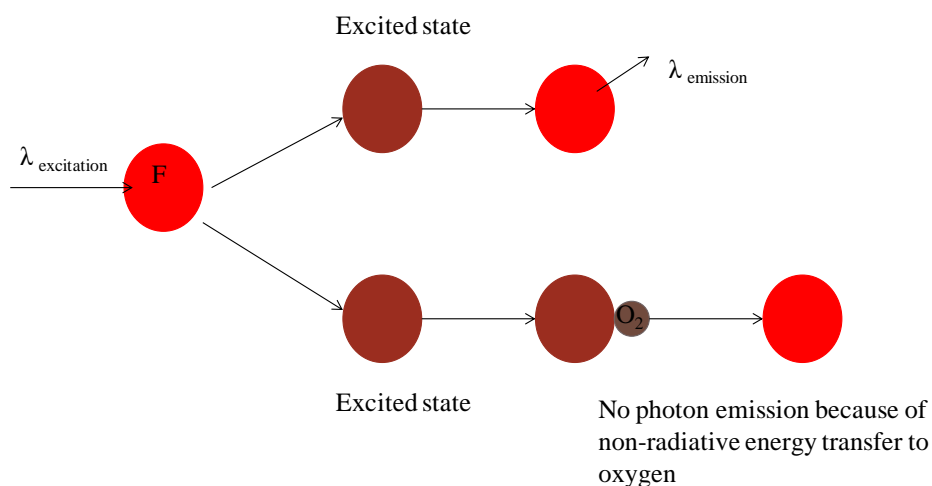
Figure 1.1. Dynamic fluorescence quenching of a fluorophore (F)

These fluorescent dyes are immobilized within an oxygen permeable matrix,
through which the excitation light source passes and excites the embedded dye within the
matrix. The most common dyes used for optical oxygen sensing are transition metal-
complex organic dyes such as ruthenium complex, metalloporphyrins such as platinum
and palladium porphyrin and fullerenes. Ruthenium complex (dichlorotris 1, 10-
phenanthroline ruthenium (II) hydrate) is widely used as an oxygen sensitive dye because
of its excellent properties such as long-term photostability, reversible oxygen quenching,

etc. This complex excites at 470nm wavelength and emits light around 600nm. The quenching mechanism is explained in detail using the underlying equations (1) and (2).

$$D \ + \ h\nu \longrightarrow D^* \longrightarrow D \ - \ h\nu' \qquad (1)$$

$$D \ + \ h\nu \longrightarrow D^* + \ O_2 \longrightarrow D + \ O_2^* \qquad (2)$$

Where D, D* represents fluorescence dye at ground and excited state respectively, O_2, O_2^* represents oxygen molecule at ground and excited state respectively, hν represents the energy illuminated from the light source @ 470nm wavelength and hν' represents energy emitted @ 600nm wavelength. Equation (1) describes the fluorescence property of a fluorophore when excited at a particular wavelength while equation (2) describes the deactivation of the dye in presence of a quencher molecule during which energy is being transferred to the quencher. This luminescence intensity is correlated to oxygen concentration using Stern-Volmer equation as follows:

$$\frac{I_0}{I} = \frac{\tau_0}{\tau} = \frac{\Phi_0}{\Phi} = 1 + K_{SV}[O_2] \qquad (3)$$

$$K_{SV} = k\tau_0 \qquad (4)$$

Where I_0, τ_0, Φ_0 indicates fluorescence intensity, lifetime and phase shift in the absence of oxygen and I, τ, Φ indicates fluorescence intensity, lifetime and phase shift in the presence of oxygen and $[O_2]$, K_{sv}, k indicates oxygen concentration, Stern-Volmer constant and quencher rate coefficient, respectively. I_0/I represent the ratio of fluorescence intensities with and without oxygen which is linearly proportional to oxygen concentration.

1.1.2.1. Absolute intensity sensing. Absolute luminescence intensity measurement for two-dimensional oxygen analysis is a straight forward method using

spectrometer where emitted light at a particular wavelength is measured with the help of optical filters for selective measurement of emission wavelength. Optical filter helps in decreasing the intensity of excitation light from the detection light. It is challenging to use absolute intensity for long-term monitoring because of intensity drift from the LED source and also due to photo bleaching or leaching of the fluorophore but is still advantageous than any other methods because of its simplicity of the equipment.

  1.1.2.2. Time-resolved sensing. To overcome the drifting issues of intensity method, two different time-resolved techniques have been developed: lifetime and phase shift. Lifetime represents the time for luminescence decay when excitation light is being switched off and phase shift represents time delay from sinusoidal excited wave because of decay lifetime as shown in figure 1.2. As seen in equation (3), the ratio of life time or phase shift in the absence of oxygen to the presence of oxygen is linearly proportional to oxygen concentration. The advantages of this time domain measurement over intensity domain include no detector shift, no effect on lifetime because of change in optical path, leaching of the dye, concentration of the dye, etc. All these drawbacks are solved with this time domain or frequency domain sensing [8].
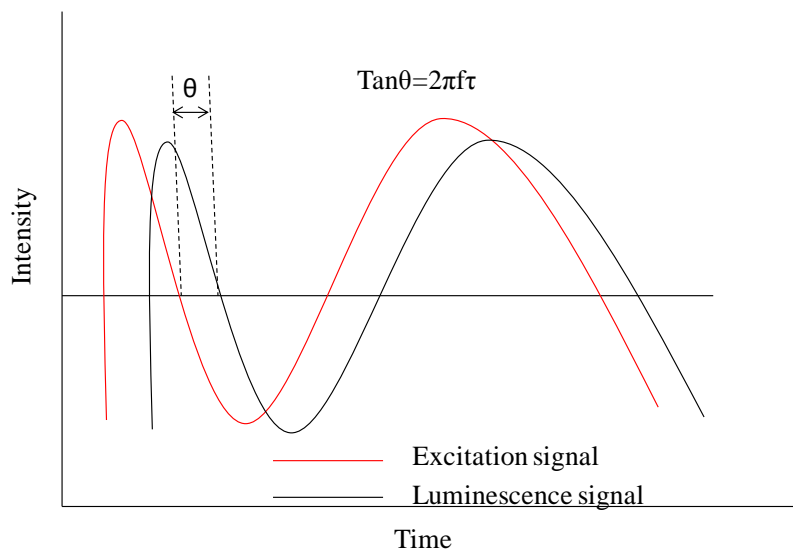
Figure 1.2. Principle of phase fluorometric technique (after[8])

1.2. OPTICAL HUMIDITY SENSORS

1.2.1. Various Methods of Humidity Sensing. Humidity is one of the major environmental quantities being measured for various biological industrial and commercial applications. It has its own diverse range of applications as mentioned below [9].

- Automotive

- Food Processing

- Meteorological

- Semiconductor

- Building and construction

- Medical and health

Based on these wide applications, various humidity measuring techniques are being applied. The basic conventional techniques for humidity sensing include mechanical hygrometer, chilled mirror hygrometer, wet and dry bulb psychrometer, etc.

These techniques exploit the basic principles of expansion and contraction with respect to humidity, optical signal reflection with respect to condensation on the mirror surface and latent heat transfer with respect to water evaporation, respectively. But miniaturized humidity sensors had an advantage over conventional sensing because of their reliability, compactness and low cost. The transduction techniques include sensors based on the change of electrical properties such as resistance and capacitance, sensors based on change in refractive index, fiber-optic humidity sensors based on absorbance measurements and fluorescence measurements and so on, as summarized in table 1.1 [10-12].

Table 1.1. Overview of transduction techniques for miniaturized humidity sensors (after[10])

Technique	Design	Particulars	Output	Materials
Optical	Fabry-Perot resonator	Contactless high-T measurement	Light-intensity	SiO_2, TiO_2
Gravimetric	Integrated	Resonant sensor, Post-CMOS processed	Frequency	Al, polyimide
Capacitive	Integrated	CMOS post-processing	Capacitance	Polyimide
Optical, Gravimetric	Miscellaneous	Materials investigation	Light, frequency	Nafion®
Capacitive	Parallel plate	Bulk device, 1st PS humidity sensor	Capacitance	Au, PS (p^+-type)
Capacitive, Optical	Membrane, IDE, two heaters, T-sensors	Multifunctional device	Capacitance, resistance, intensity of light	SiO_2, Si_3N_4
Capacitive	Miscellaneous	3D-modelling and design studies	Capacitance	Polymers
Gravimetric	IDE, SAW	Quartz substrate	Frequency	Polymers, TiO_2, Pd
Gravimetric	IDE	Thick-film technology	Frequency	Quartz, polyimide
Hygrometric	Membrane	CMOS post-processing	Voltage	Polyimide
Gravimetric	Cantilever	Resonant sensor	Frequency	PVDF
Hygrometric	Membrane	Piezoresistive detection, modelling	Voltage	Polysilicon, Polyimide
Capacitive	IDE	Materials investigation	Capacitance	Al_2O_3 on SiO_2/Si
Optical	Fibre-optic	Multi-point measurements	Light-intensity	-
Capacitive	Integrated	Humidity-sensitive FET	Voltage	Au, TiO_2
Thermoelectric	Differential bridge design	Measurement of absolute humidity	Voltage (current supply)	Pt, Ta_2O_5
Gravimetric	IDE, SAW	Dew point, Peltier cooling	Frequency	Al, ST-Quartz
Optical	Thin-film	Materials investigation	Light-intensity	PS (p-type)
Optical	Fibre-optic	Surface-plasma-based device	Transmission	-

All the above developed techniques have their own advantage regarding high sensitivity and good reliability along with some drawbacks including the use of bulky equipments for humidity detection, instability caused by temperature during long-term use of these techniques, high power consumption, etc. But optical humidity sensors even with these limitations have a capability of sensing low-level moisture levels [12]. This capability made it superior to its counterparts, with further developments in fiber-optic based humidity sensors. They involve the usage of colorimetric materials embedded on the surface of a fiber core with change in refractive index or optical intensity transmittance as their sensing mechanism as sown in table 1.2.

Table 1.2. Overview of transduction techniques for optical humidity sensors (after [12])

Design	Materials	Output	Remarks
Fiber-optic	$CoCl_2$	Intensity of light	Surface-plasma-based device
Fiber-optic	Agarose gel	Optical power	Sol-gel deposition
Spectrometer	-	Spectrometer	Frequency modulation
Movable window	Black hair	Voltage	Photodiode for conversion
Fluoroscent	Optode membrane	Transmission	Fluoroscent optosensor
UV-VIS spectra	Complex-forming dyes	Absorbance	Charge transfer complex-forming dyes
Fiber-optic	PMMA	Transmission	U-shaped probe
Fluoroscent	Optode membrane	Transmission	Fluoroscent optosensor
Optical reflection	Peltier device	Voltage	Dew point sensing
Fabry-Perot interferometer	Photoacoustic cell	Wavenumber	Photoacoustic
Fiber-optic	Nano-like MgO	Transmission	U-shaped probe
Luminescence spectra	Pt(II) double salt materials	Wavelength	Vaporluminescent

The table 1.2 above summarizes different designs of optical humidity sensors used in lab-scale technologies. Different fluorescent dyes embedded within different polymer matrices are being used as humidity sensitive materials with change in their absorbance or transmittance properties. The common optic-fiber sensors employed the immobilization of the humidity sensitive dye such as cobalt chloride (II) hexahydrate ($CoCl_2$ $6H_2O$) on the core surface of the fiber.

       1.2.2. Cobalt Chloride as Humidity Sensor. A special class of humidity sensors works on the principle of absorption/color changes in different humidity sensitive dyes like cobalt (2+) chloride hexahydrate, cobalt thiocyanate, crystal violet, methylene blue, rhodamine, etc. Cobalt (2+) chloride hexahydrate has been used widely for humidity analysis because of its wide range of color change at different relative humidity (%RH). Anhydrous $CoCl_2$ is blue in color with an absorption spectrum at around 490nm where completely hydrated $CoCl_2.6H_2O$ is ruby-red crystalline in nature with peak around 410-550nm. Spectral absorption of the dye at different relative humidities was measured. Pure cobalt chloride cannot be used as humidity sensor by itself because of its powdery nature when dry. Therefore different hydrophilic polymer matrices are used to embed $CoCl_2$ within the matrix, which then can be exposed to different humidity environment. The polymer matrices used include poly vinyl alcohol (PVA), poly methyl methacrylate (PMMA), gelatin, Poly-2-hydroxyethyl methacrylate (poly-HEMA), etc.

1.3. TROPIC RESPONSES OF PLANT ROOTS

Plants are sessile organisms, sensitive to various environmental factors with complex growth processes during their whole lifecycle. Plant root behavior depends on the nature of rooting medium through which nutrients are being transferred to the plant

root. Growth of plant roots through this media is a very complex process because of numerous biotic and abiotic stresses applied on the root system. For plants to grow and survive in different environmental conditions, roots must be capable of detecting nutrients in the media and grow in that direction. The zone of interaction within the soil is referred as rhizosphere which varies spatially along the root axis. The root tip response to environmental stimuli by directed growth plays a major role in plant development. With the help of these tropic responses of roots, plants can help themselves during environmental risks such as drought conditions. The major tropic responses include gravitropism, hydrotropism, oxytropism and thigmotropism important for the survival of terrestrial plants. Although many studies were conducted on gravitropic response, much area of other tropism is less explored [13].

1.3.1. Hydrotropism. Hydrotropism indicates the detection of moisture and orientation of plant roots towards soil moisture. The degree of root curvature depends on the intensity of humidity gradient formed in the vicinity of plant root. Different hydrostimulants were used for analyzing the hydrotropic behavior of plant roots. Figure 1.3 compares the direction of root curvature with respect to humidity gradient in active sensor and induced artifact process. The curvature of the root arises from the turgor potential of the root cells by moisture gradient in induced artifact. The turgor potential of the root cells tend to increase in the direction of higher water potential which leads to root curvature towards dry soil in induced artifact phenomenon and natural curvature towards higher water potential in an active-sensor phenomenon.
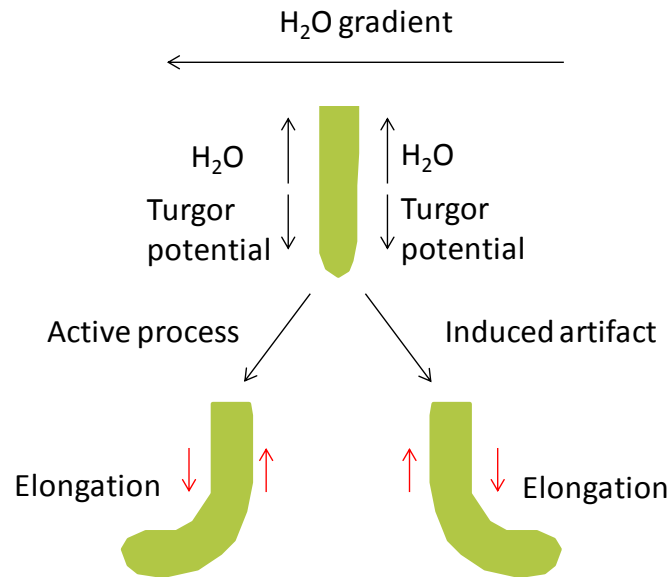
Figure 1.3. Diagram demonstrating the difference between an active sensor-based hydrotropic response and an induced artifact (after [13])

1.3.2. Oxytropism. Oxytropism indicates the detection of oxygen and orientation of plant roots towards higher oxygen levels. The degree of root curvature depends on the intensity of oxygen gradient formed in the vicinity of plant root. Figure 1.4 compares the direction of root curvature with respect to oxygen gradient in active sensor and induced artifact process. The curvature of the root arises from the differential metabolic activity of the root cells by oxygen gradient in induced artifact. This leads to root cells expansion in the direction of higher oxygen concentration which results in root curvature towards lower oxygen concentration in induced artifact phenomenon and natural curvature towards higher oxygen concentration in an active-sensor phenomenon.
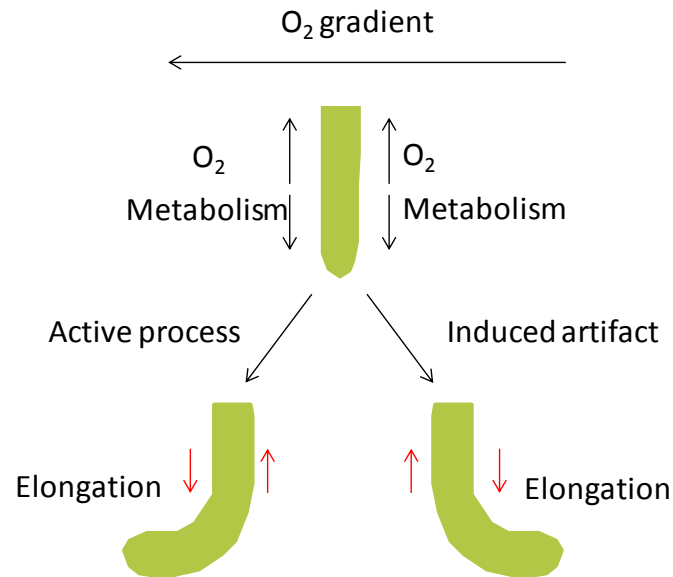
Figure 1.4. Diagram demonstrating the difference between an active sensor-based oxytropic response and an induced artifact (after [13])

The above figures conclude that the tropic responses happen naturally without any induced artifact. Classical approach of creating tropic responses includes agar plate treatment where spatial control was done on the order of a millimeter. Therefore work was done creating devices which helps in maintaining chemical stimuli around a plant root. Takahashi et al. worked on investigating different devices for studying hydrotropic response on plant roots pea, corn, etc. In this work moist cheese cloth was used as hydrostimulant and calcium chloride inside the chamber for purging 83% RH. Humidity within the chamber was measured using a probe but humidity analysis near the plant root was not analyzed [14-17]. Porterfield et al. worked on a meso-scale fluidic device fabrication for creating oxygen gradient around the plant root. Even in this work, oxygen measurement near the plan root was not specified [18]. Therefore, this work is focused on creating a meso-scale fluidic device for studying the oxytropic and hydrotropic behavior on plant roots with integrated chemical sensors within the device. Integrated humidity

sensors were embedded within the fluidic device for measuring humidity gradient formed near the plant root. Porphyrine complex embedded within Ethyl Cellulose (EC) was employed as oxygen detection mechanism. A charge-coupled device (CCD) camera was used for both chemical sensing and structural imaging of the plant root.

REFERENCES

[1]   Gerhard Holst, Bjorn Grunwald, "Luminescence lifetime imaging with transparent oxygen optodes," Sensors and Actuators B, 74, 78-90, 2001

[2]   Paul Hartman, Werner Ziegler, Gerhard Holst, Dietrich W. Lubbers, "Oxygen flux flurorescence lifetime imaging," Sensors and Actuators B, 38-39, 110-115, 1997

[3]   Gregor Liebsch, Ingo Klimant, Bernhard Frank, Gerhard Holst, Otto S. Wolfbeis, "Luminescence lifetime imaging of oxygen, pH, and carbon dioxide distribution using optical sensors," Applied spectroscopy, 54(4), 549-559, 2000

[4]   J. Park, W. Hong, C-S. Kim, "Color intensity method for hydrogel optical sensor array," IEEE Sensors Journal, 10 (12), 1855-1861, 2010

[5]   X-d. Wang, R. J. Meier, M. Link, O. S. Wolfbeis, "Photographing Oxygen Distribution," Angewandte Chemie - International Edition, 49 (29), 4907-4909, 2010

[6]   J. Park, C-S. Kim, "A simple oxygen sensor imaging method with white light-emitting diode and color charge-coupled device camera," Sensor Letters, 9 (1), 118-123, 2011

[7]   Samuel Shin, "Cost-effective oxygen gas sensor via fluorescence quenching", Proceedings of the Multi-Disciplinary Senior Design Conference

[8]   C.McDonagh, C.Kolle, "Phase fluorometric dissolved oxygen sensor", Sensors and Actuators B, 74, 124-130, 2001

[9]   T.L.Yeo, T.Sun, "Fiber-optic sensor technologies for humidity and moisture measurement",   Sensors and Actuators A, 144, 280-295, 2008

[10] Z.M.Rittersma, "Recent achievements in miniaturized humidity sensors-a review of transduction techniques", Sensors and Actuators A, 96, 196-210, 2002

[11] Zhi Chen, Chi Lu, "Humidity sensors: A review of materials and mechanisms", Sensor Letters, 3, 274-295, 2005

[12] Chia-Yen Lee, Gwo-Bin Lee, "Humidity sensors: A review", Sensor Letters, 3, 1-15,   2005

[13] Yoav Waisel, Amram Eshel, "Environmental sensing and directional growth of plant roots", Plant roots-the hidden half, third edition, Marcel Dekker Inc., 2002

[14] Hideyuki Takahashi, "Hydrotropism and its interaction with gravitropism in roots", Plant and Soil, 165, 301-308, 1994

[15] Hideyuki Takahashi, T.K.Scott, "Intensity of hyrdostimulation for the induction of root hydrotropism and its sensing by the root cap", Plant , Cell and Environment, 16, 99-103, 1993

[16] Hideyuki Takahashi, Hiroshi Suge, "Root hydrotropism of an agravitropic pea mutant, ageotropum", Physiological Plantarum, 82, 24-31, 1990

[17] Hideyuki Takahashi, Tom K.Scott, "Hydrotropism and its interaction with gravitropism in maize roots", Plant Physiology, 96, 558-564, 1991

[18] D.Marshall Porterfield, Mary E.Musgrave, "The tropic response of plant roots to oxygen:oxytropism in Pisum sativum L.", Planta, 206, 1-6, 1998

PAPER

I.   WET OXYGEN QUANTIFICATION USING DISPLAY SCREEN WITH RGB BACKLIGHTS AND CCD CAMERA

ABSTRACT

Optical oxygen imaging is essential in monitoring two-dimensional analysis of oxygen distribution. Two easily accessible optical devices were used for oxygen analysis to demonstrate the feasibility of an innovatively simple method. A light panel screen with light-emitting diode (LED) backlight was used as a light source to excite a luminophore responsive to oxygen. Meso-scale fluidic sensor platform was prepared using porphyrin complex as the sensitive dye embedded within ethyl cellulose (EC) polymer matrix. Green LED light uniformly displayed from the light panel excited the dye film to exhibit two-dimensional luminescence distribution corresponding to wet gaseous oxygen. A color charge-coupled device (CCD) camera was used as a photodetector for registering oxygen images and analyzing the oxygen contents quantitatively. This simple oxygen imaging enables in meso-scale area distribution with ubiquitous optical devices.

Keywords

oxygen, porphyrin, ethyl cellulose, color camera, charge coupled device, light panel

1. INTRODUCTION

Optical oxygen sensors are in well-known demand in many areas of biological oxygen monitoring because of their ability for non-destructive detection and miniaturization. Most of these optical sensors work on the principle of quenching where oxygen quenches the luminescence emitted from a luminophore. These luminescent dyes are immobilized within an oxygen permeable matrix, through which the excitation light source passes and excites the embedded dye within the matrix. The basic detection mechanism for measuring the quenched intensity from a luminophore includes spectrum analysis using a spectrometer mostly for one-dimensional quantification.

In order to conduct two-dimensional oxygen distribution, various optical imaging techniques have been developed. These optical imaging techniques are based on either luminescence intensity measurements or luminescence lifetime measurements which include both frequency domain and time domain [1-3]. In recent past, several simple imaging techniques based on colorimetry have been reported utilizing familiar photodetector equipment including charge-coupled device (CCD) or complementary metal-oxide-semiconductor (CMOS) color cameras [4-7]. It has been successfully demonstrated that these familiar devices can be effectively used for both quantitative and qualitative determination of oxygen contents.

Furthermore, our previous works reported the use of rather unconventional light sources, including white LED and computer display screen, as the excitation source for oxygen determination [8-9]. A blue light peak (around 480 nm) from these sources was utilized to excite the ruthenium-complex which is an oxygen-responsive luminophore.

Especially, the display screen proved to be an excellent candidate for large-area oxygen mapping due to its ability of uniform illumination of light over a wide area. With this background information, in this work we demonstrate the use of a green light panel as an excitation source for both one-dimensional qualitative and two-dimensional quantitative oxygen determination.. Platinum porphyrin complex, Pt(II) octaethylpophyrine (PtOEP), sensor films were immobilized in ethyl cellulose polymer matrix and excited using green light (around 530 nm) displayed from the light panel. Color images were taken at different oxygen concentrations using the color CCD camera which were later modified for quantitative oxygen analysis.

2.   MATERIALS AND SENSOR FABRICATION

2.1. Materials

Platinum porphyrine complex, Pt (II) Octaethylpophyrine (PtOEP), used for oxygen detection was ordered from Frontier Scientific in powder-form.   The polymer matrix used for embedding the luminophore was ethyl cellulose (EC) which has high permeability towards oxygen. Toluene, tetrahydrofuran (THF) and ethanol were used as solvents for preparing the oxygen sensor cocktail. Wet oxygen and nitrogen gases were prepared by purging dry gases with 99.9% purity through deionized water bottles.

2.2. Preparation of precursor solution

The sensor cocktail was prepared based on a method from a previous study done by others [10] where luminophore concentration has been optimized for better and linear sensitivity. A stock solution of 10mg porphyrine complex in 10ml of THF was prepared and stirred for 30 minutes. The polymer matrix was prepared by mixing 3g of EC in 6ml of ethanol and 24ml of toluene and stirred for 30minutes. The final oxygen sensor

cocktail was prepared by mixing sensor stock solution into the polymer matrix. The final precursor solution was stirred for 30minutes before pipetting 6ml of the solution onto a glass plate. The solution was spin coated at 300rpm for 10 seconds to obtain a uniform sensor film (approximately 25 microns) on the surface of the glass plate. The glass plate with oxygen sensor was placed overnight in dark at room temperature for curing of the polymer matrix.

2.3. Sensor platform fabrication

A Y-junction sensor platform has been fabricated for creating a mixed flow within the main channel of the Y-junction using two glass plates (75x50mm) and a rubber spacer (around 2mm thick). The layout and cross-section of the sensor platform is represented in Figure 1. The rubber spacer was glued to the glass plates using epoxy glue. Two gas influxes of different oxygen ratios were purged through the Y-junction which helps in investigating oxygen mapping through the main channel. The same set up was used for sensor calibration by swapping the outlet and inlet ports.
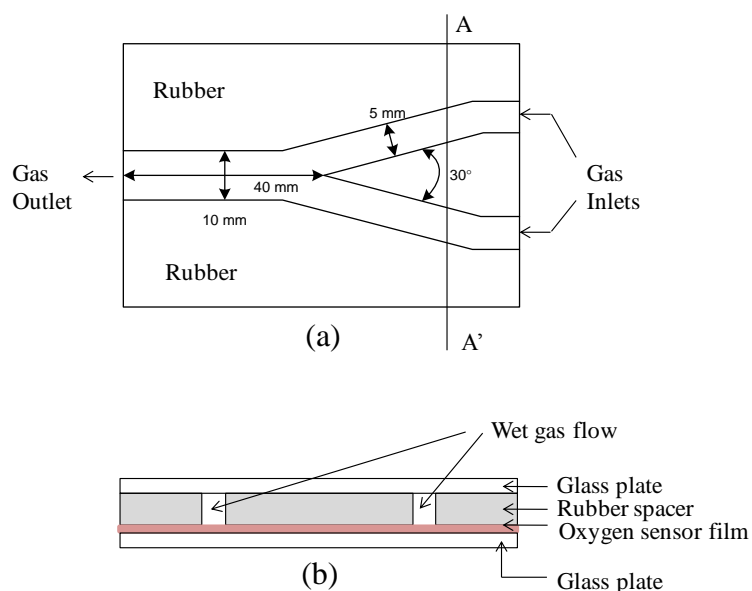
Figure 1. Oxygen sensor platform (a) Layout (b) cross-sectional view (A-A')

3. EXPERIMENTAL SET UP

3.1. Excitation source (RGB LED Light Panel)

The traditional excitation source has been replaced by a RGB LED light panel (5x5", Green Led Lighting Solutions Inc.) with different led backlighting and light intensity around 2000-5000 cd/m^2. Green light with wavelength range of 500-560nm with a peak around 530nm was turned on to excite the fluorophore. A dimmer switch was used to manipulate the light intensity with respect to oxygen sensitivity. No color filter layers were used for light production because of pure green led's placed within the panel.

3.2. Photodetector (Color CCD Camera)

The fluorescence emission from the oxygen sensor around 600nm has been recorded using a color CCD camera (Sony alpha350 DSLR camera with 14.2 Megapixel). These CCD cameras have their own in-built filter arrays of three different elemental colors – red, green and blue called Bayer filters. The arrangement and working of these Bayer filter array is as shown in figure 2.
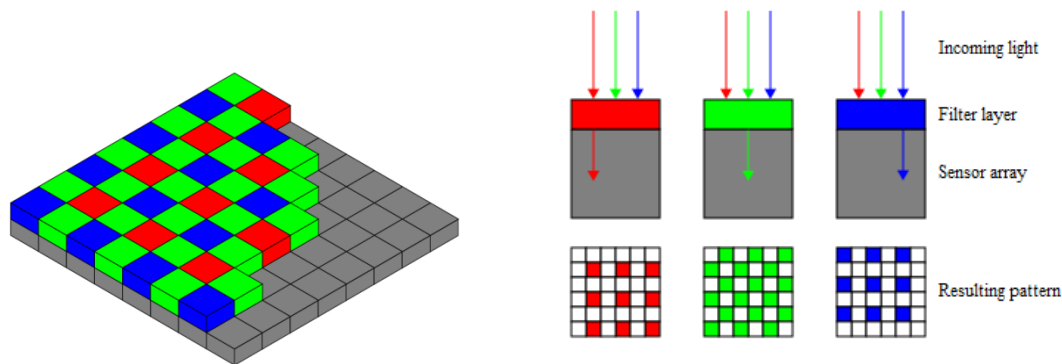
Figure 2. Bayer filter arrangement (after [14])

Each filter passes its own specific wavelength through it and the photo sensor senses it in terms of voltage with respect to the number of photons passed. As the

emission intensity changes with respect to oxygen concentration, the CCD chip detects the change from low to high red intensity using its bayer filter array. All the camera settings were selected manually in order to avoid any image correction done automatically by the camera. The parameter shutter speed (represents the exposure time of the photosensor to light) has to be carefully selected in order to obtain good sensitivity. The sensitivity is also affected with the ISO (International Standards organization) number. Higher the ISO number, higher the sensitivity of the photosensor. Table 1 below summarizes the camera settings used for further sensor characterization.

Table 1. Optimized camera conditions

Parameters	ISO	Shutter speed	White balance	F number	Focus
Setting values	200	0.1"	Sunlight	5.6	Focused

The red pixel of the CCD chip is also sensitive over blue and green wavelengths as shown in the figure 3 below. Therefore to avoid the influence of the strong green excitation light source on the emission light intensity, a long pass filter (OG610, cut-off wavelength 610nm, Thorlabs) was placed in front of the detection mechanism (color CCD camera). This filter also helps in minimizing any stray light interference with the sensitivity of the sensor.
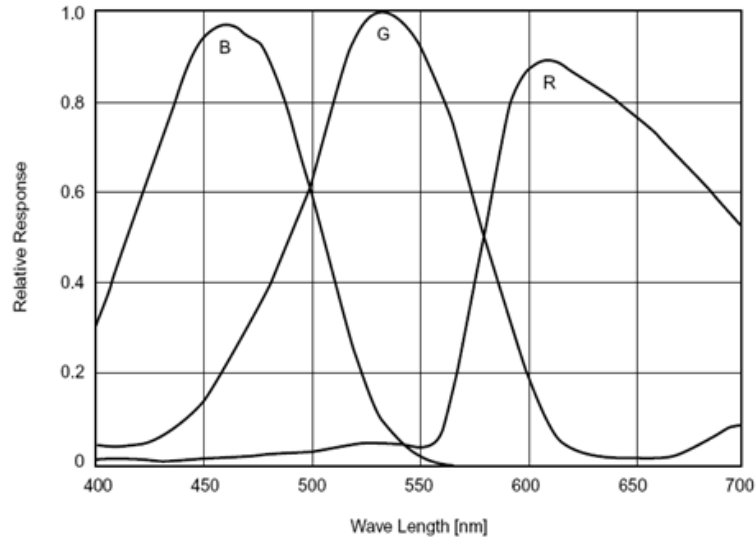
Figure 3. General spectral sensitivity characteristics of a CCD chip in a digital camera (after [15])

3.3. Measurement set up

The red pixel of the CCD chip is also sensitive over blue and green wavelengths .

Therefore to avoid the influence of the strong green excitation light source on the

emission light intensity, a long pass filter (OG610, cut-off wavelength 610nm, Thorlabs)

was placed in front of the detection mechanism (color CCD camera) as shown in Figure

2. This filter also helps in minimizing any stray light interference with the sensitivity of

the sensor. A 1.5mm thick glass plate was placed on the surface of the light panel using

elastic spacers of 5mm thick and then the sensor platform was attached to the surface of

the glass plate. Direct contact of the sensor platform with the light panel was avoided to

minimize any changes caused due to thermal radiation from the screen. The color CCD

camera was placed 1 foot away from the light panel and the whole set up was placed in a

dark chamber to minimize any stray light effects. Different ratios of wet oxygen and wet

nitrogen gases were purged through the sensor platform for further sensor calibration and

characterization. The green light was turned on for at least two minutes followed by

taking ten pictures continuously for averaging the sensitivity of ten images.
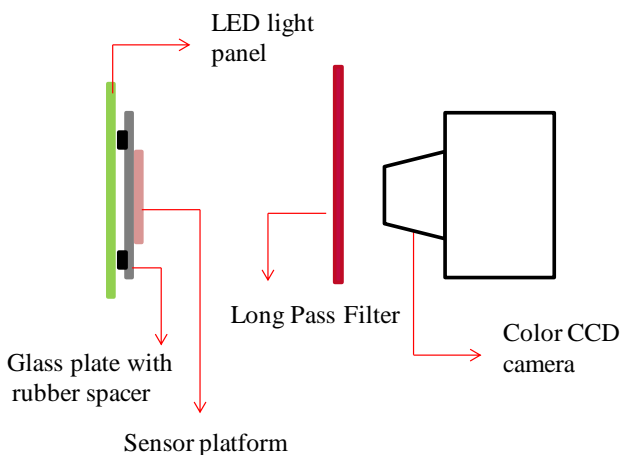
Figure 4. Measurement set up for oxygen analysis using color CCD camera and LED light panel

3.4. Image processing using MATLAB

The luminescence intensity measured is correlated to oxygen concentration using

Stern-Volmer equation as follows:

$$\frac{I_0}{I} = \frac{\tau_0}{\tau} = \frac{\Phi_0}{\Phi} = 1 + K_{SV}[O_2]$$

(1)

$$K_{SV} = k\tau_0$$

(2)

where I, τ, Φ indicates luminescence intensity, lifetime and phase shift in the presence of

oxygen (the subscript "o" denotes the absence of oxygen) and $[O_2]$, K_{sv}, k indicates

oxygen concentration, Stern-Volmer constant and quencher rate coefficient, respectively.

I_0/I represent the ratio of luminescence intensities with and without oxygen which is

linearly proportional to oxygen concentration. MATLAB codes were written for

analyzing the images taken at different oxygen concentrations and reconstructing the

oxygen distribution images. In order to minimize the noise levels, averaging techniques

was employed by taking average of ten images taken continuously at different oxygen

concentrations. Red extraction analysis has been carried out on all the images taken at

different oxygen concentrations. Stern-Volmer equation helps in quantitative oxygen

analysis. The whole sensor platform was saturated with nitrogen (i.e. 0% oxygen) and

imagers were taken which represents I_0 of equation (1) and then different arbitrary

oxygen concentrations were purged through the sensor platform which represents I of

equation (1).   According to Stern-Volmer equation, I_0/I needs to be calculated for

qualitative oxygen analysis and so the images taken at I_0 and I were divided with respect

to each pixel number using Matlab. A five-point calibration at 0%, 5%, 10%, 15% and

21% was carried out for quantitative oxygen analysis within the sensor platforms.

4. RESULTS AND DISCUSSION

4.1. Screen spectrum analysis

Before characterizing the oxygen sensor, it has to be confirmed that the green led

light from the panel can excite the porphyrine complex with the exact wavelength.

Therefore, three elemental LED color (red, green, blue) emissions were characterized

before sensor analysis using an optical fiber spectrometer (USB2000-FLG, Ocean optics).

The spectrum analysis of the three colors is represented in figure 5 below. The

porphyrine-complex fluorophore gets excited for fluorescence emission around 535 nm.

From the figure above, we can conclude that the green light from the LED light panel

spans in the range of 500-560nm with a peak around 530nm which matches with the

excitation wavelength of porphyrine complex.
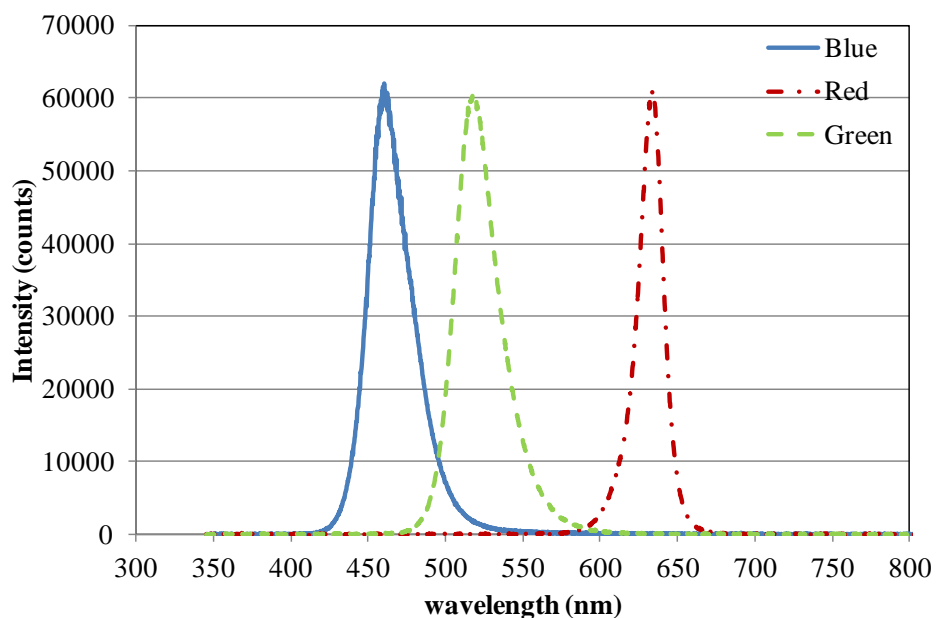
Figure 5. Spectra of three primary colors (blue, green and red) displayed by the LED panel

4.2. Oxygen sensor analysis using spectrometer

Different oxygen concentrations were purged through the sensor platform and analyzed using spectrometer to confirm the adoption of green light panel as excitation source. The sensor platform was placed over the light panel along with the long pass filter (cut-off around 610nm).The reflection probe was placed such that the emission light was detected without any interference of the excitation light using the spectrometer. As mentioned in the previous section, five different wet oxygen concentrations were flushed through the sensor platform for atleast 15minutes each. All the gases were bubbled through water before purging into the sensor platform. To avoid any intensity based errors, normalized intensity (Io/I) was plotted against different oxygen concentrations as shown in figure 6 where Io represents the intensity at 0% oxygen and I represent the related intensity at specific oxygen concentration.
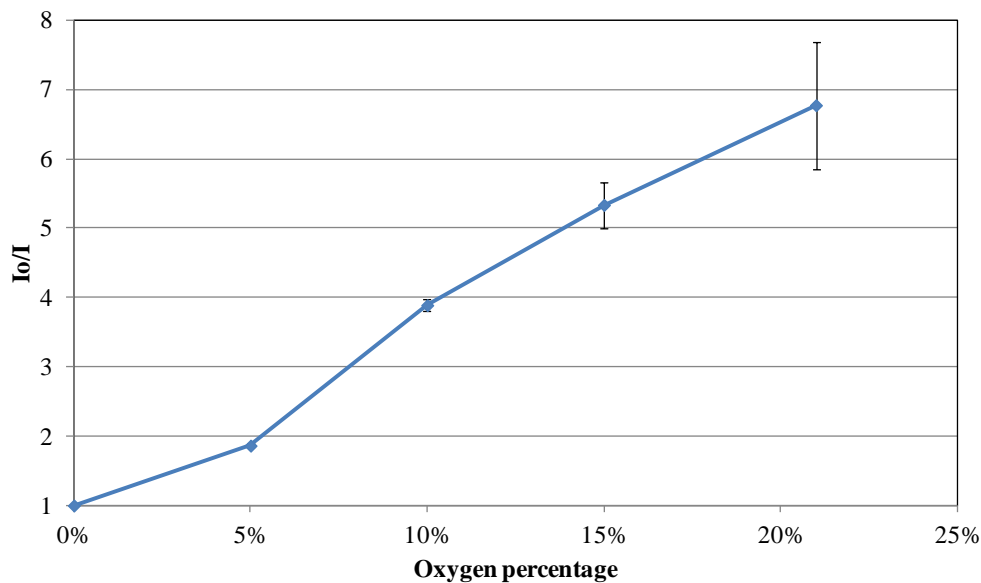
Figure 6. Stern-Volmer plot of the oxygen sensor using spectrometer (n=4)

According to the Stern-volmer equation, a linear relationship should be exhibited between I_0/I and oxygen concentration which has been attained. This confirms that the LED light panel can be used to excite the porphyrine sensor complex resulting in good sensitivity. Time response of the sensor membrane was also plotted along with its reversibility as shown in figure 7 with different oxygen gases purged for 5minutes each with time response of about 2-3 minutes on average.
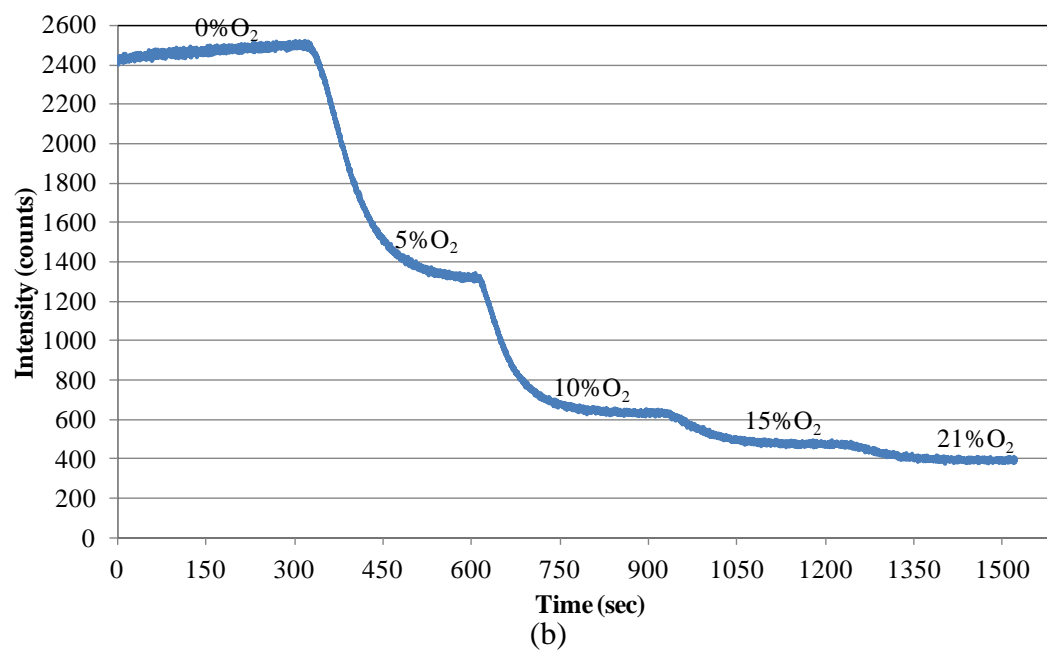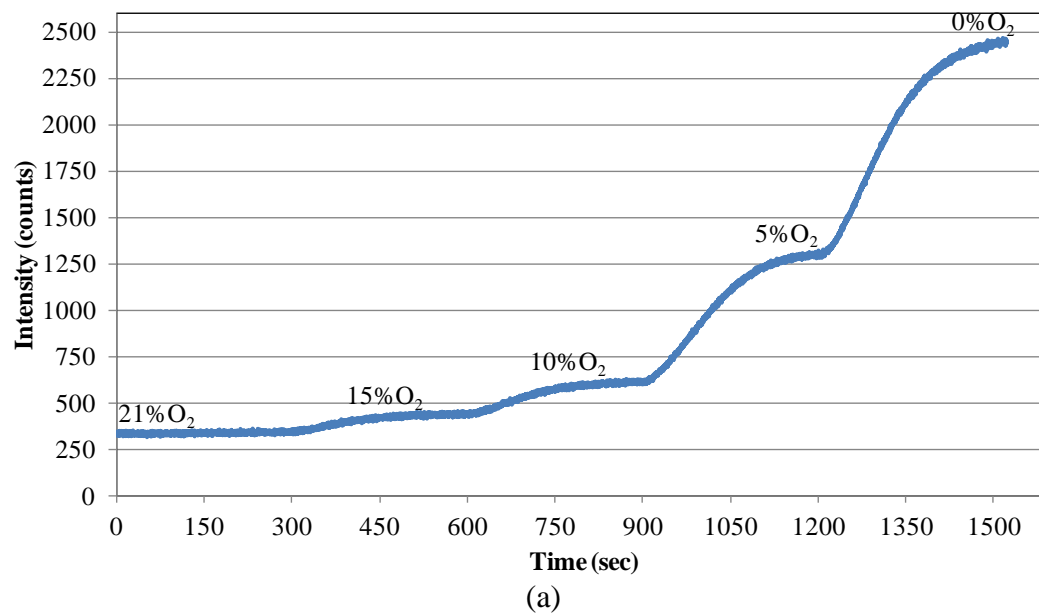
Figure 7. Time response of the sensor membrane (a) from 21% O_2-0% O_2 (b) from 0% O_2-21% O_2

4.3. Oxygen sensor analysis using color CCD camera

Different oxygen concentrations were flushed through the sensor platform for at least 20minutes each and images taken with different camera settings which include the ISO number and the shutter speed. Red intensity images were extracted from the color images. The camera was able to capture the grid lines on the light panel which affected the sensitivity of the sensor membrane. Therefore four different region of interest (ROI around 30x30 pixels each) were analyzed and averaged within each and every image. Figure 8 represents the sensitivity of the sensor with different camera settings. All the camera settings were selected manually in order to avoid any image correction done automatically by the camera. The parameter shutter speed has to be carefully selected in order to obtain good sensitivity.
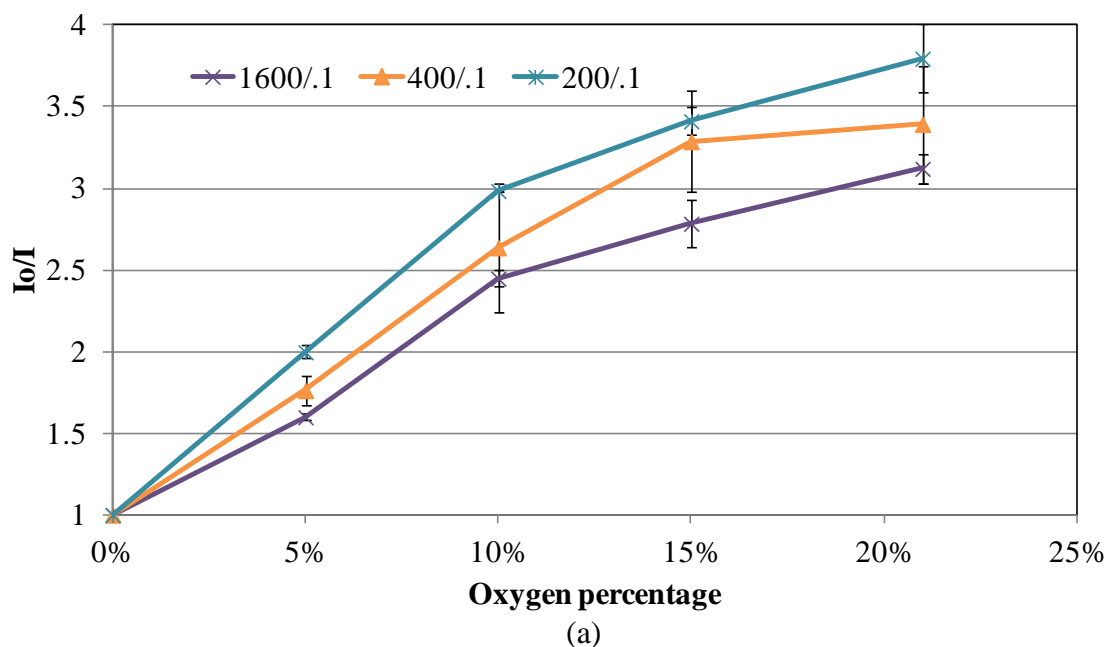
(a)

Figure 8. Stern-Volmer plots with respect to different camera settings (a) Different ISO conditions with shutter speed 0.1sec (b) Different shutter speed with ISO 200 (n=3)
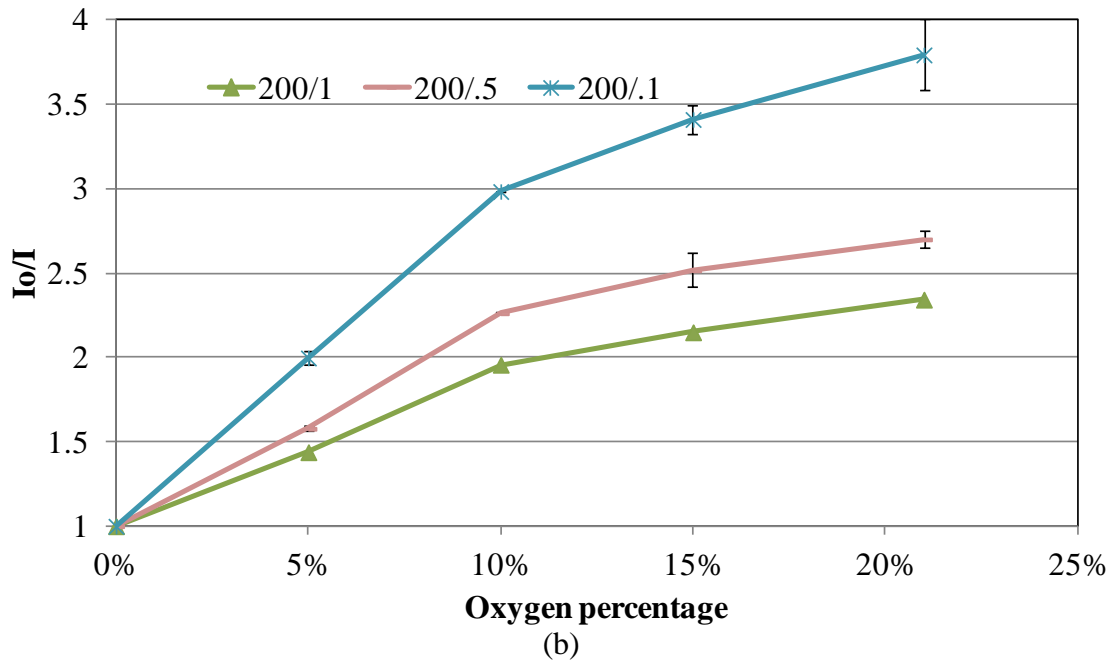
Figure 8. Stern-Volmer plots with respect to different camera settings (a) Different ISO conditions with shutter speed 0.1sec (b) Different shutter speed with ISO 200 (n=3) (cont.)

The sensitivity is also affected with the ISO (International Standards organization) number as shown in figure 8 (a). Higher the ISO number, higher the sensitivity of the photosensor. From the above figure, ISO 200 and shutter speed of 0.1sec has been set as the optimized conditions for better and linear sensitivity. The camera was set with these conditions for further experiments.

4.4. Y-junction sensor platform for two-dimensional analysis

An oxygen distribution image of the Y-junction sensor platform was created using different oxygen concentrations (0% and 21% O_2). Figure 9(a) indicates the average red intensity image of the ten color images of the completely nitrogen saturated Y-junction channel (the reference image Io) and figure 9(b) indicates the average red intensity image of the ten color images with saturated with 0% O_2 from top channel and 21% O_2 from

bottom channel (the image I). An oxygen gradient has been created using laminar flow within the Y-junction sensor platform by purging both 21% and 0% wet oxygen gases at a specific flow rate (30SCCM) through the inlets.
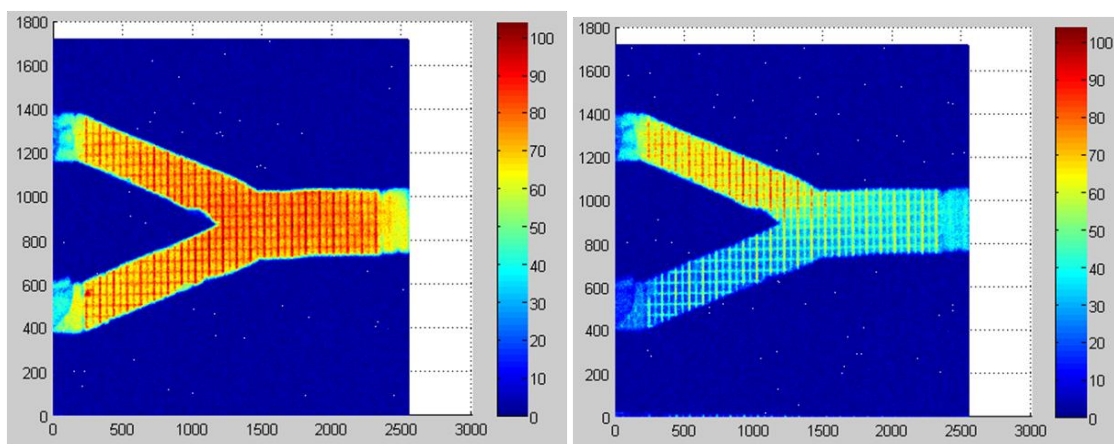
(a)

(b)
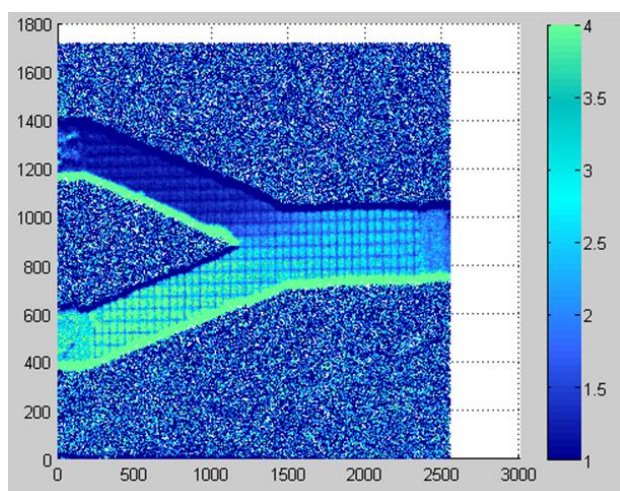
(c)

Figure 9. False color images of the sensor platform (a) Red intensity image with nitrogen from both the inlets (Io) (b) Red intensity image with 0% oxygen from top channel and 21% oxygen from bottom channel (I) (c) Stern-Volmer image (Io/I)

Difference in colors in figure 9 (a) and (b) represents the change in red intensity value with respect to change in oxygen level. Stern-Volmer image (Io/I) helps in nullifying any of the errors and gives qualitative distribution of the sensor platform. Quantitative oxygen analysis can also be done using the calibration data provided in figure 8. MATLAB coding helps in quantitative oxygen analysis is mentioned in Appendix A. From the figure it can be clearly stated that oxygen mapping can be easily done in a large distribution of area. This oxygen mapping helps in monitoring the behavior of various biological tissues, plant roots at different oxygen concentrations otherwise in the same environment.

5. CONCLUSIONS

Wet oxygen analysis has been successfully completed using two easily accessible optoelectronic devices as excitation source and detection mechanism. The porphyrine complex was successfully excited with a light panel yielding to two-dimensional oxygen analysis. The color CCD camera has great potential in capturing and sensing the required emission range. The obtained image was processed by conventional image processing technique to extract the red color component from the original RGB color image and quantitatively relate it to the oxygen level within the channel. The red color analysis employed with Stern-Volmer equation using MATLAB helped in error rectification. The proposed technique is expected to serve as a simple instrumentation setup and detection mechanism for oxygen imaging in meso-scale fluidic device with embedded oxygen sensors for potential applications to biologically investigate oxytropic response of small plant roots.

REFERENCES

[1] Gerhard Holst, Bjorn Grunwald, "Luminescence lifetime imaging with transparent oxygen optodes," Sensors and Actuators B, 74, 78-90, 2001

[2] Paul Hartman, Werner Ziegler, Gerhard Holst, Dietrich W. Lubbers, "Oxygen flux fluorescence lifetime imaging," Sensors and Actuators B, 38-39, 110-115, 1997

[3] Gregor Liebsch, Ingo Klimant, Bernhard Frank, Gerhard Holst, Otto S. Wolfbeis, "Luminescence lifetime imaging of oxygen, pH, and carbon dioxide distribution using optical sensors," Applied Spectroscopy, 54(4), 549-559, 2000

[4] P. C. Thomas, M. Halter, A. Tona, S. R. Raghavan, A. L. Plant, S. P. Forry, A Noninvasive thin film sensor for monitoring oxygen tension during in vitro cell culture, Analytical Chemistry, 81, 9239-9246, 2009

[5] J. Park, W. Hong, C-S. Kim, "Color intensity method for hydrogel optical sensor array," IEEE Sensors Journal, 10 (12), 1855-1861, 2010

[6] X-d. Wang, R. J. Meier, M. Link, O. S. Wolfbeis, "Photographing Oxygen Distribution," Angewandte Chemie - International Edition, 49 (29), 4907-4909, 2010

[7] L. Shen, M. Ratterman, D. Klotzkin, I. Papautsky, Use of a low-cost CMOS detector and cross-polarization signal isolation for oxygen sensing, IEEE Sensors Journal, 11(6), 1359-1360, 2011

[8] J. Park, C-S. Kim, "A simple oxygen sensor imaging method with white light-emitting diode and color charge-coupled device camera," Sensor Letters, 9 (1), 118-123, 2011

[9] Sanghan Park, Satya Achanta, Chang-Soo Kim, Intensity-based oxygen imaging with a display screen and a color camera, Sensors & Actuators B-Chemical, 164, 101-108, 2012

[10] Tai-Sheng Yeh, Chen-Shane Chu, "Highly sensitive optical fiber oxygen sensor using Pt(II) complex embedded in sol-gel matrices", Sensors and Actuators B, 119, 701-707, 2006

[11] Li Shen, Michael Ratterman, "A CMOS optical detection system for point-of-use luminescent oxygen sensing", Sensors and Actuators B, 155, 430-435, 2011

II.   COLORIMETRIC HUMIDITY ANALYSIS USING DISPLAY SCREEN AND COLOR CAMERA

ABSTRACT

Humidity is one of the major environmental quantities being measured for various biological, industrial and commercial applications. Cobalt chloride (II) hexahydrate particles embedded within a hydrophilic PVA matrix has been employed for humidity sensor fabrication in this work. Familiar optoelectronic devices, charge coupled device (CCD) color camera and liquid crystal display (LCD) screen were utilized in this work. As the cobalt chloride particles change from blue when dry to pink when humid, the CCD chip can detect this color. After the images were taken with different backlight displayed on the LCD screen, they were analyzed using ImageJ software for red color extraction analysis. This optical humidity sensor is expected to be useful in two-dimensional humidity sensing over a meso-scale without any use of bulky equipment.

Keywords

Colorimetric analysis, Charge coupled device (CCD), Liquid crystal display (LCD), Cobalt chloride (II) hexahydrate (CoCl2.6H2O), Poly vinyl alcohol (PVA), Humidity sensor

1. INTRODUCTION

Humidity is one of the major environmental quantities being measured for various industrial and commercial applications. Based on the application, various humidity measuring techniques are being applied. The basic conventional techniques for humidity sensing include mechanical hygrometer, chilled mirror hygrometer, wet and dry bulb psychrometer, etc. These techniques exploit the basic principles of expansion and contraction with respect to humidity, optical signal reflection with respect to condensation on the mirror surface, latent heat transfer with respect to water evaporation, respectively [1].

Miniaturized humidity sensors however had a demand over conventional sensing because of their potential advantages such as reliability, compactness, good sensitivity, small hysteresis, no temperature dependence, high shelf life time, fast response time and low cost. The transduction techniques include sensors based on the change of electrical properties such as resistance and capacitance and optical sensors based on change in refractive index, absorbance and fluorescence emission and so on. All the above developed techniques have their own advantage regarding high sensitivity and good reliability along with some drawbacks including the use of bulky equipments for humidity detection, instability caused by temperature during long-term use of these techniques, high power consumption, etc [1-4].

Optical humidity sensors even with these limitations have a capability of sensing low-level moisture levels. This capability made it superior to its counterparts, with further developments in fiber-optic based humidity sensors. They involve the usage of colorimetric materials embedded on the surface of a fiber core with change in refractive

index or optical intensity transmittance as their sensing mechanism. The common fiber-optic sensors employed the immobilization of the humidity sensitive dye such as cobalt chloride (II) hexahydrate ($CoCl_2.6H_2O$) on the core surface of the fiber. As a known fact, anhydrous cobalt chloride is blue in color with an absorption spectrum at around 490nm, while completely hydrated cobalt chloride hexahydrate is ruby-red crystalline in nature with peak around 410-550nm. The spectral absorption of the core material was measured at different relative humidities [5-13].

Based on the above background, we focused on developing a humidity sensor based on simple colorimetric imaging mechanism which can avoid the usage of bulky equipments and has a simple measurement set up. In this work, a color CCD camera was used as photodetector for humidity analyzing and a LCD screen was utilized for uniform light illumination over a meso-scale area. As the cobalt chloride particles change from blue when dry to pink when humid, the CCD chip can detect its change. The major advantage of using LCD screen as light source includes the presence of three different primary color filters within these LCD screens which forms different colors. After the images were taken with different backlight, they were analyzed using ImageJ software. This software helps in analyzing a color image by extracting the primary colors red, green and blue intensity from the actual RGB image. Cobalt chloride (II) hexahydrate particles embedded within a PVA matrix has been employed in this work.

2. EXPERIMENTAL

2.1. Materials

The humidity sensitive dye, cobalt chloride (II) hexahydrate ($CoCl_2.6H_2O$) was ordered from Sigma-Aldrich. The polymer, polyvinyl alcohol (PVA, high molecular weight, Sigma-Aldrich), was used for hydrogel membrane fabrication because of its swelling behavior in presence of humidity. Maelic acid (MA) used as a cross linker for PVA hydrogel fabrication was also purchased from Sigma-Aldrich. Pure cobalt chloride embedded within the PVA matrix tends to leach out from the polymer matrix. Therefore, in order to decrease the leaching of the dye, cobalt chloride was physically adsorbed onto fumed silica particles (Cab-O-Sil EH-5, Mozel) which are hydrophilic in nature. Pure deionized water was used as solvent for preparing the polymer solution as well as loading cobalt chloride particles onto silica. To decrease the leaching of free cobalt chloride particles (which did not adsorb onto silica particles), the hydrogel membrane formed was sandwiched using a thin dialysis sheet (Membrane dialysis, Scienceware). All the chemicals were used without any further purification.

2.2. Hydrogel membrane formation

Pure PVA hydrogel fabrication has been followed as mentioned in reference (14). 10 wt% aqueous PVA was prepared by stir heating the mixture at $80^{o}C$ for 30minutes. A clear viscous PVA solution was formed and different concentrations of the cross linker MA were added to this solution. Small amounts of 1M conc. H_2SO_4 were added to the polymer solution which plays the role of a catalyst. The whole mixture was stirred for 30minutes. Table 1 indicates the optimization of the concentration of the cross linker.

From the summarized table below, 0.45g of MA has been used for further experimentation because of its uniform membrane formation.

Table 1. Composition of the polymer with different cross linker concentrations

SL No.	Cross Linker (Maelic Acid-MA) in grams	PVA in grams	PVA to MA ratio	Membrane properties
1	0.2	1	5:1	Uniform membrane but high degree of leaching
2	0.45	1	20:9	Uniform membrane with less degree of leaching
3	0.7	1	10:7	Less degree of uniformity
4	1	1	1:1	Non-uniform membrane with lots of aggregation spots indicating high amounts of MA
5	2	1	1:2	Same as above

Aqueous cobalt chloride solution was prepared where the concentration of the dye was maintained three times the weight of the polymer PVA. Small amounts (3g) of the dye was dissolved in 10ml deionized water and stirred for 30minutes. To decrease leaching of the dye, fumed silica particles (0.6g) were added to the aqueous cobalt chloride solution and stirred overnight for complete physical adsorption of the dye onto

silica particles. The concentration of silica particles has been optimized based on the degree of saturation of the aqueous solution. After 24hrs of stirring the solution turned dark pink in color indicating complete adsorption. An aliquot of this solution (6ml) was mixed with the polymer solution prepared as mentioned above and stirred for atleast 30-40 minutes. The whole solution was spin coated on a glass slide at 300 rpm for 20 seconds for uniform sensor fabrication. A thin transparent membrane was formed on the glass slide which was then placed on the hot plate at $40^{o}C$ for at least 6-8 minutes unless the membrane turned into a uniform blue color indicating complete evaporation of water. Now a thin dialysis sheet was laminated on the surface of the membrane immediately for effective adhering of the sheet on the membrane. This dialysis sheet is hydrophilic in nature and the molecular weight cut-off (MWCO) of the membrane has been selected such a way that the cobalt chloride particles present beneath the sheet will not be able to leach out through the dialysis sheet. The sandwiched membrane was then heated to $80^{o}C$ for 2 hours for thermal esterification to take place between the polymer and the cross linker which helps in embedding the dye within the cross linked PVA polymer.

2.3. Instrumentation and characterization

Because of the hydrophilic nature of the dialysis sheet and the swelling property of the polymer PVA in presence of moisture, cobalt chloride particles sandwiched within the membrane tend to change their color with respect to the moisture being permeated through the membrane. This color change has been recorded using a color CCD camera (Sony alpha350 DSLR camera with 14.2 Megapixel).
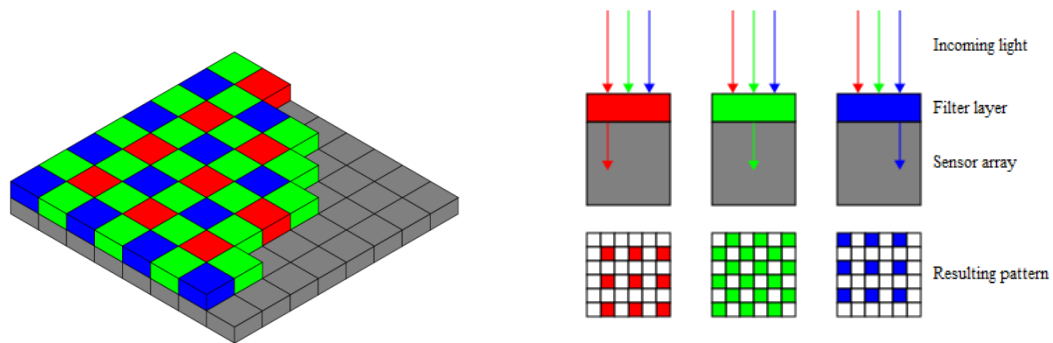
Figure 1. Bayer filter arrangement (after [15])

The arrangement and working of the Bayer filter array built-in within the camera is shown in figure 1. Each filter passes its own specific wavelength through it and the photo sensor senses it in terms of voltage with respect to the number of photons passed. As the cobalt chloride particles change from blue when dry to pink when humid, it would be easy for the CCD chip to detect the change from blue to pink using its bayer filter array. All the camera settings were selected manually in order to avoid any image correction done automatically by the camera. The parameter shutter speed (represents the exposure time of the photosensor to light) has to be carefully selected in order to obtain good sensitivity. The sensitivity is also affected with the ISO (International Standards organization) number. Higher the ISO number, higher the sensitivity of the photosensor Table 2 below summarizes the camera settings used for further sensor characterization.

Table 2. Optimized camera conditions

Parameters	ISO	Shutter speed	White balance	F number	Focus
Setting values	800	0.02"	Sunlight	5.6	Focused

Therefore images of the sensor film at different relative humidities were taken using the CCD camera with optimized conditions under uniform light illumination. The light illumination on the sensor should be uniform all over the surface for error minimization. In this work, uniformly illuminating white fluorescence light as a light source was replaced by a TFT LCD screen because of wide area measurements and more uniform light illumination on each pixel of the image taken at different humidities. The major advantage of using these LCD screen as light source because of three different primary color filters within these LCD screens which forms 16,777,216 different colors with 24-bit RGB color space. So, these different colors displayed on the LCD screen help in taking images without the use of any color filters. After the images were taken with different backlight, they were analyzed using ImageJ software. This software helps in analyzing a color image by extracting the primary colors red, green and blue intensity from the actual RGB image.

3. RESULTS AND DISCUSSION

3.1. Humidity sensor sensitivity

Humidity sensor platform was fabricated using 1mm thick rubber spacers and attached to the LCD screen surface with elastic spacers (5mm thick). Direct contact of the

sensor platform with the LCD screen was avoided to minimize any changes caused due to thermal radiation from the screen. The color CCD camera was placed $1 - 1.5$ feet away from the LCD screen and the whole set up was placed in a dark chamber to minimize stray light effects. A dehumidifier was used to produce different gases of different humidity. Images were taken at room humidity (50% RH) with different backlights and then 0% and 100% RH gases were purged through the sensor and images taken with respect to time. Images taken were analyzed using image J for color analysis. Sensitivity based on different backlights and different color extractions was analyzed and plotted as shown in figure 2.
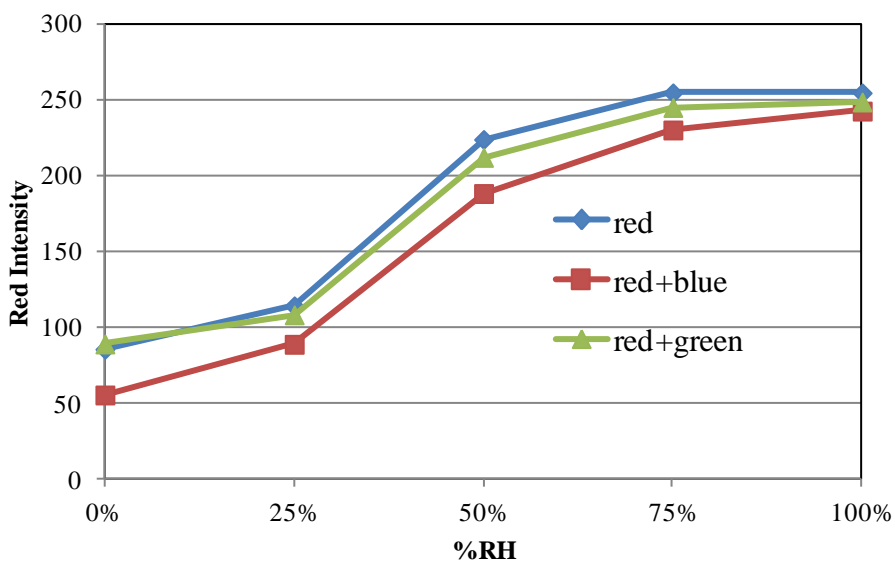
(a)

Figure 2. Sensor sensitivity with different backlights and (a) red extraction (b) green extraction (c) blue extraction

(b)

(c)
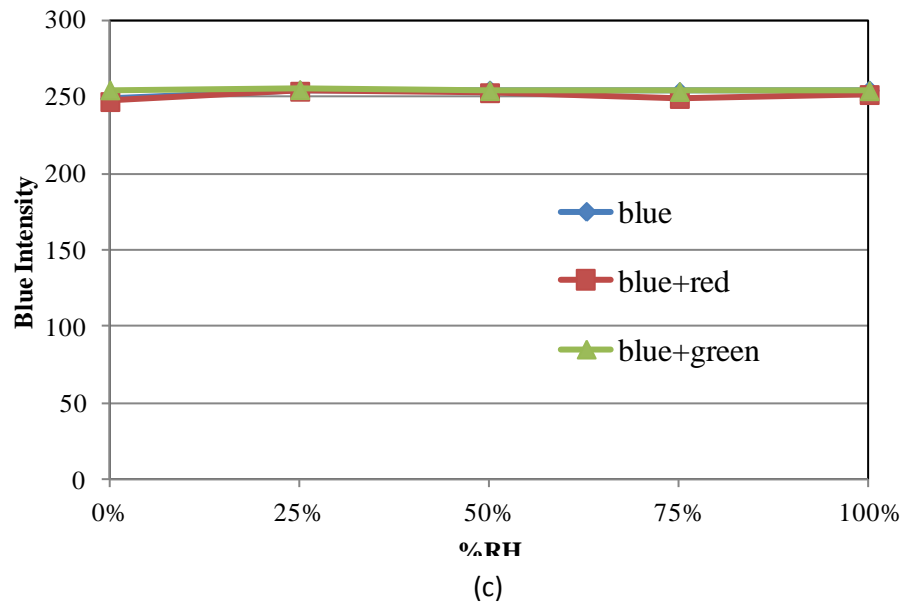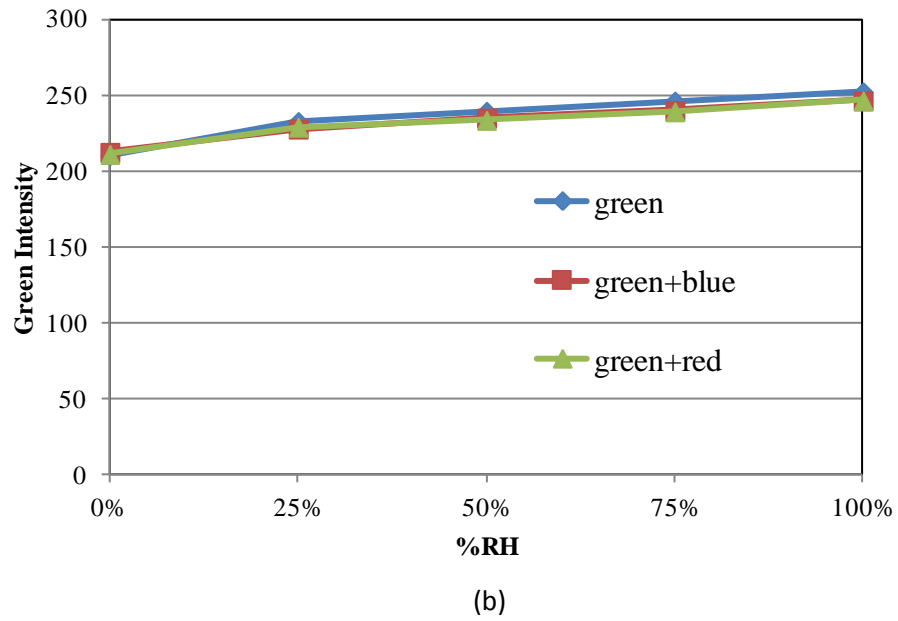
Figure 2. Sensor sensitivity with different backlights and (a) red extraction (b) green extraction (c) blue extraction (cont.)

Based on the above graphs, it is clear that red extraction of images taken at

red+blue, red and red+green backlights gives good sensitivity with respect to %RH.

Therefore, further experiments were carried out with red+blue backlight along with red

extraction analysis. Image J analysis of images with red color extraction is shown in table

3 below.

Table 3. Histogram analysis at different % RH using image J
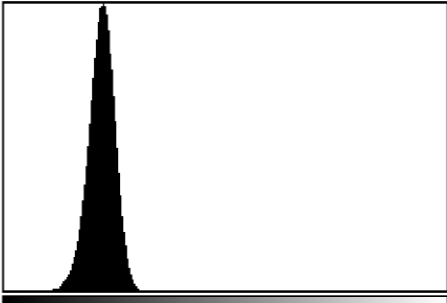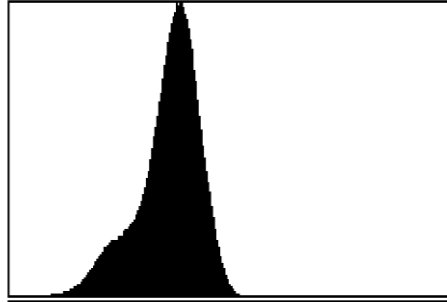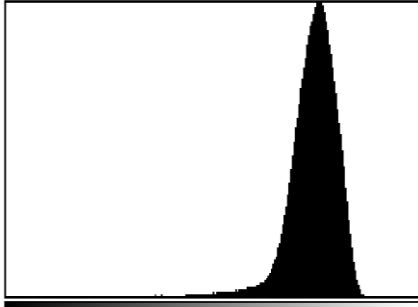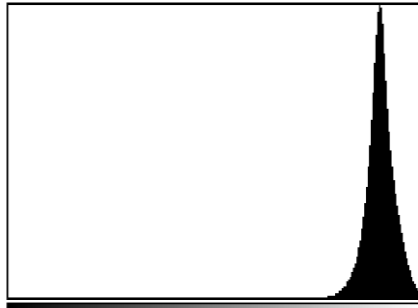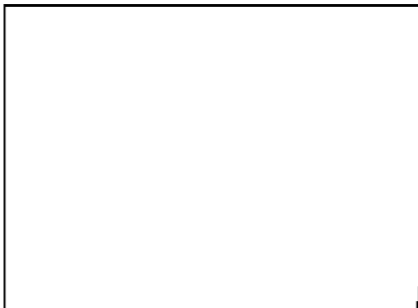
RGB image	Humidity (%RH)	Red extraction with image J	Histogram for red extraction analysis
	Dry (0% RH)		0 255 Count: 962136 Min: 0 Mean: 55.749 Max: 135 StdDev: 7.967 Mode: 57 (51846)
	25% RH		0 255 Count: 1542240 Min: 0 Mean: 89.117 Max: 248 StdDev: 18.345 Mode: 96 (42678)

Table 3. Histogram analysis at different % RH using image J (cont.)

	50% RH		
			Count: 1414224 Min: 3 Mean: 188.379 Max: 229 StdDev: 20.210 Mode: 195 (43769)
	75%RH		
			Count: 1434240 Min: 63 Mean: 230.221 Max: 255 StdDev: 10.260 Mode: 230 (83632)
	100%RH		
			Count: 450432 Min: 190 Mean: 242.643 Max: 255 StdDev: 4.011 Mode: 243 (48301)

The histogram analysis represented in table 3 shows the difference in mean value of red intensity from each image taken at different %RH.

3.2. Time response and reversibility

A cycle of experiments were conducted from dry to humid and finally back to dry condition to analyze the response time and the repeatability of the sensor. Based on figure 3, we can conclude that this humidity sensor gives repeatable results. Different humid gases were purged for about 12-13 hrs each for complete saturation with almost 30-45 minutes of response time on average. The prepared membrane has a very good sensitivity within the range of 25-75%RH with very low sensitivity between 75-100%RH.
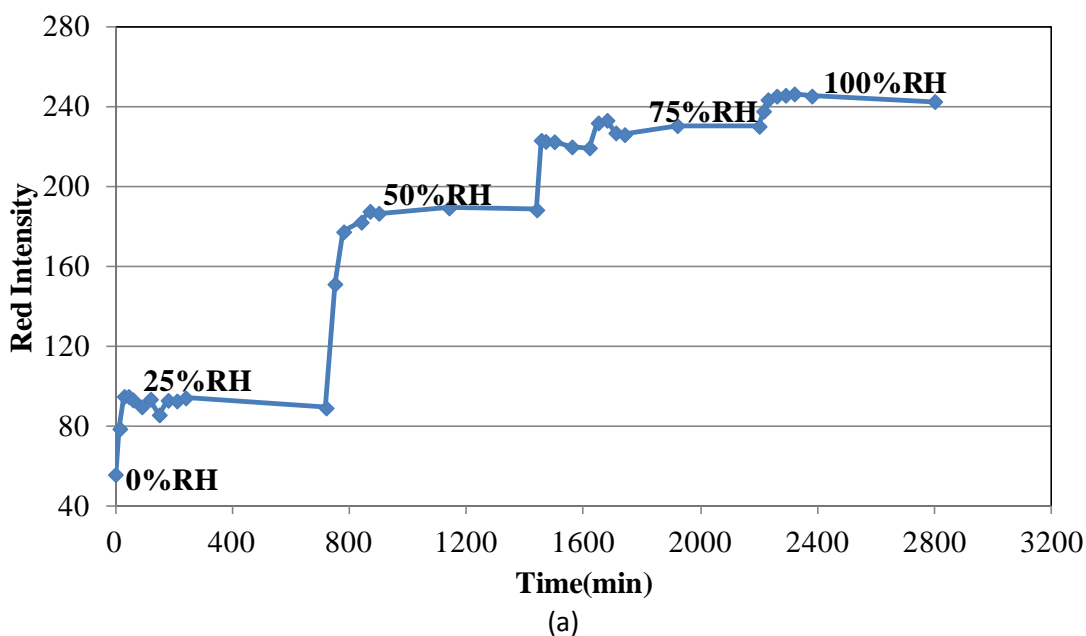
(a)

Figure 3. Time response of the sensor membrane with red+blue backlight and red extraction using image J (a) from 0-100%RH (b) from 100-0%RH

(b)
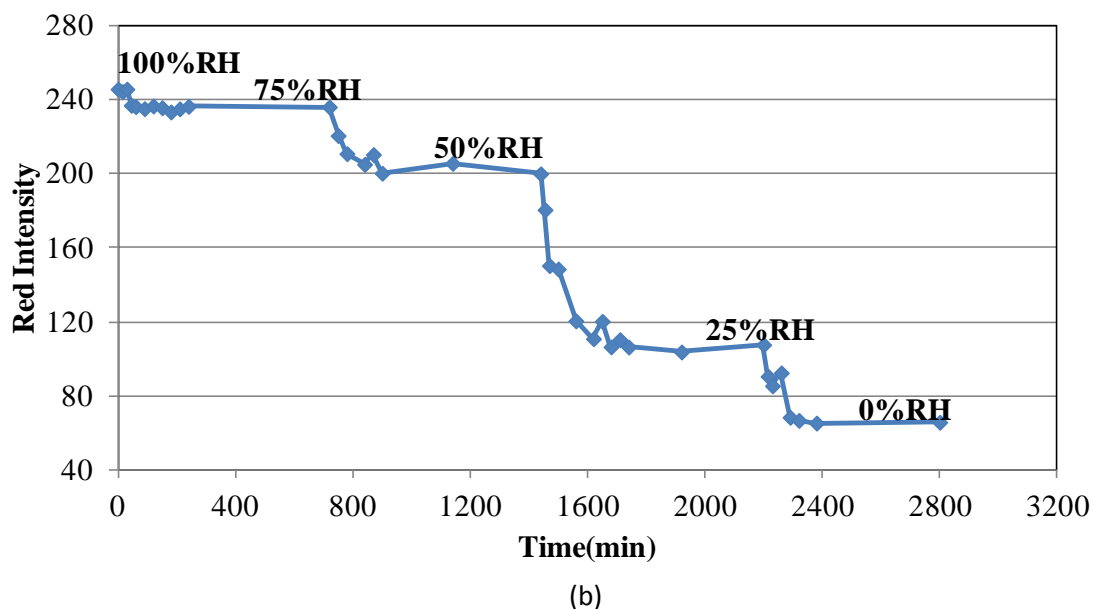
` Figure 3. Time response of the sensor membrane with red+blue backlight and red extraction using image J (a) from 0-100%RH (b) from 100-0%RH (cont.)

4. CONCLUSIONS AND FUTURE WORK

Based on our data, the sensor fabricated has very good sensitivity with red extraction analysis using image J. A humidity sensor using hydrogel PVA membrane has been fabricated and a different humidity analysis method was used which did not have any bulky detection mechanism and had compatibility with two-dimensional humidity analysis. The amount of leaching of the dye has been decreased by sandwiching the humidity membrane using a thin dialysis sheet which is hydrophilic in nature. The sensitivity of the membrane was increased by changing the backlights of the LCD screen and the shutter speed of the color CCD camera. The fabricated membrane has a good response time based on the cycle of experiments carried out using 5-point calibration (0%-25%-50%-75%-100% RH). Future work includes modification of the membrane to increase its sensitivity within the range of 75-100%RH for future biological applications.

REFERENCES

[1]   T.L.Yeo, T.Sun, "Fiber-optic sensor technologies for humidity and moisture measurement", Sensors and Actuators A, 144, 280-295, 2008

[2]   Z.M.Rittersma, "Recent achievements in miniaturized humidity sensors-a review of transduction techniques", Sensors and Actuators A, 96, 196-210, 2002

[3]   Zhi Chen, Chi Lu, "Humidity sensors: A review of materials and mechanisms", Sensor Letters, 3, 274-295, 2005

[4]   Chia-Yen Lee, Gwo-Bin Lee, "Humidity sensors: A review", Sensor Letters, 3, 1-15, 2005

[5]   Candido Bariain, Ignacio R.Matias, "Optical fiber humidity sensor based on a tapered fiber coated with agarose gel", Sensors and Actuators B, 69, 127-131, 2000

[6]   Jesus M.Corres, Francisco J.Arregui, "Sensitivity and optimization of tapered optical fiber humidity sensors by means of tuning the thickness of nanostructured sensitive coatings", Sensors and Actuators B, 122, 442-449, 2007

[7]   Shinzo Muto, Akihiko Fukasawa, "Optical detection of moisture in air and in soil using dye doped plasti fibers", Japanese Journal of Applied Physics, 29, 1023-1025, 1990

[8]   Francisco J.Arregui, Zuri Ciaurriz, "An experimental study about hydrogels for the fabrication of optical fiber humidity sensors", Sensors and Actuators B, 96, 165-172, 2003

[9]   Francisca Boltinghouse, Kenneth Abel, "Development of an optical relative humidity sensor. cobalt chloride optical absorbency sensor study", Analytical Chemistry, 61, 1863-1866, 1989

[10]   Sunil K.Khijwania, Kirthi K.Srinivasan, "Performance optimized ptical fiber sensor for humidity measurement", Optical Engineering, 44, 2005

[11]   C.M.Tay, k..Tan, "Humidity sensing using plastic optical fibers", Microwave And Optical Technology Letters", 43, 387-390, 2004

[12]   Pabitra Nath, Hidam Kumarjit Singh, "Cobalt chloride doped polymer film for relative humidity measurement", Sensors and Transducers, 91, 127-133, 2008

[13]   M.E.Solomon, "The use of cobalt salts as indicators of humidity and moisture", Annals Of Applied Biology, 32, 75-85, 1945

[14]   Penny Martens, Jennifer Blundo, "Effect of poly (vinyl alcohol) macromer chemistry and chain interactions onhydrogel mechanical properties", Chemistry Of Materials, 19, 2641-2648, 2007

[15]   http://en.wikipedia.org/wiki/Bayer_filter, Bayer Filter, August 2009

III.   RHIZOBOX WITH TWO-DIMENSIONAL HYDROSTIMULANT AND EMBEDDED SENSORS TO INDUCE ROOT HYDROTROPIC RESPONSES

ABSTRACT

The root tip response to environmental stimuli by directed growth plays a major role in plant development. With these tropic responses of roots, plants can help themselves during environmental risks such as drought conditions. Therefore, study on plant root tropic responses gives valuable information on plant metabolic activity and development. Rhizobox with two-dimensional hydrostimulant placed at a particular angle was fabricated with embedded humidity sensors within the device to study the effect of tropic responses on small plant roots of corn. A flow of humid gases was purged through the main channel of the device for creating humidity gradient with the help of a hydrostimulant placed at an angle of 45 degrees. Hydrotropic behavior of corn roots was analyzed along with humidity gradient quantification using color charge-coupled device (CCD) camera for both imaging of the plant root and profiling of humidity distribution. Custom-made humidity sensors were used for colorimetric analysis of humidity in the range of 50-100%RH. Red extraction analysis of color images using imageJ gives excellent interpretation of humidity profiling with respect to extracted red intensity values. Successfully created and analyzed the humidity gradient which resulted in root orientation because of hydrotropic response indicating the effectiveness of this device for further biological applications.

1. INTRODUCTION

Growth of plant roots through rooting media is a very complex process because of numerous biotic and abiotic stresses applied on the root system. For plants to grow and survive in different environmental conditions, roots must be capable of detecting nutrients in the rooting media and grow in that direction. The zone of interaction within the soil is referred as rhizosphere which varies spatially along the root axis. The root tip response to tropic responses by directed growth plays a major role in plant development. With the help of these tropic responses of roots, plants can help themselves during environmental risks such as drought conditions. The major environmental stimuli include gravitropism, hydrotropism, oxytropism and thigmotropism important for the survival of terrestrial plants. Although many studies were conducted on gravitropic response, much area of other tropisms is not fully explored. Knight et al. first demonstrated the effect of gravitropism and phototropism on a monocot seedling. It was demonstrated that the hormone auxin was responsible for these kinds of tropisms [1].

Later, work has been done on determining hydrotropism where plant roots tend to grow towards higher moisture region within the rooting media. Classical approach of creating hydrotropic response includes agar plate treatment where spatial control was done on the order of a millimeter. It has been noticed that hydrotropic sensing in plant roots encountered significant biological and technological difficulties which includes the interference of gravitropism and creation of moisture gradient. But Jaffe et al. and Takahashi et al. worked on developing different hydrotropic sensing techniques to overcome these difficulties. Their work was focused on studying the hydrotropic response by creating moisture gradient within a small chamber, where moist cheese cloth

or an agar block was used as hydrostimulant placed at specified angles and calcium chloride placed inside the chamber for creating 83% RH environment. From their experiments it was concluded that the intensity of hyrdostimulation helps in neglecting the interaction of gravitropism with hydrotropism. It has also been concluded that the effect of the hydrostimulant depends on its distance from the plant root. Hydrostimulant placed at a far distance (more than few millimeters) have negligible effect on plant roots. But these experiments failed in analyzing the moisture gradient formed within the whole experimental set up [2-5].

Later the same group worked on creating moisture gradient using water potential. Agar plates with different sorbitol concentrations were placed such a way that moisture gradient was formed because of sorbitol transfer from on agar plate to the other [6-10]. Even these experiments failed in simultaneous chemical analysis along with root response.

Literature includes different ways of sensing and measuring moisture/humidity in the environment. The basic conventional techniques for humidity sensing include mechanical hygrometer, chilled mirror hygrometer, wet and dry bulb psychrometer, etc. These techniques exploit the basic principles of expansion and contraction with respect to humidity, optical signal reflection with respect to condensation on the mirror surface, latent heat transfer with respect to water evaporation, respectively. But miniaturized humidity sensors had a demand over conventional sensing because of their reliability, compactness and low cost. The transduction techniques include sensors based on the change of electrical properties such as resistance and capacitance, sensors based on change in refractive index, fiber-optic humidity sensors based on absorbance

measurements and fluorescence measurements. All these techniques have their own advantage regarding high sensitivity and good reliability along with some drawbacks including the use of bulky equipments for humidity detection, instability caused by temperature during long-term use of these techniques, high power consumption, etc. But optical humidity sensors even with these limitations have a capability of sensing low-level moisture levels. This capability made it superior to its counterparts, with further developments in fiber-optic based humidity sensors [11-14]. They involve the usage of colorimetric materials embedded on the surface of a fiber core with change in refractive index or optical intensity transmittance as their sensing mechanism. Different fluorescent dyes embedded within different polymer matrices are being used as humidity sensitive materials with change in their absorbance or transmittance properties. The common optic-fiber sensors employed the immobilization of the humidity sensitive dye such as cobalt chloride (II) hexahydrate ($CoCl_2$ $6H_2O$) on the core surface of the fiber [15-18]. A special class of humidity sensors works on the principle of absorption/color changes in different humidity sensitive dyes like cobalt (2+) chloride hexahydrate, cobalt thiocyanate, crystal violet, methylene blue, rhodamine, etc. Cobalt (2+) chloride hexahydrate has been used widely for humidity analysis because of its wide range of color change at different relative humidity (%RH). Anhydrous $CoCl_2$ is blue in color with an absorption spectrum at around 490nm where completely hydrated $CoCl_2.6H_2O$ is ruby-red crystalline in nature with peak around 410-550nm. Spectral absorption of the dye at different relative humidities was measured for humidity analysis [19-23]. Therefore, custom made cobalt (2+) chloride hexahydrate based humidity sheet (with sensing range of 50-100%RH) was used to analyze the humidity gradient formed within the fluidic device.

With this background information, we focused on creating a rhizobox for studying the hydrotropic behavior on plant roots with integrated chemical sensors within the device. The hydrostimulant was placed at an angle of 45 degrees to observe root orientation with respect to humidity. The integrated sensors help in quantitative analysis of the gradients being formed using the fluidic channels with simultaneous observation of plant behavior. A charge-coupled device (CCD) camera was used for both humidity profiling and imaging of the plant root. Custom-made humidity sensors were used for colorimetric analysis of humidity in the range of 50-100%RH. Red extraction analysis of color images using imageJ gives excellent interpretation of humidity values with respect to extracted red intensity values.

2. GERMINATION PROTOCOL

8 to 10 corn seeds (variety B73) were placed on stack of germination papers saturated with deionized water inside a petri dish. The whole set up was wrapped with a porous tape for air exchange. The petri dish was placed vertically in dark for 4-5 days until roots of length 4-5cm were formed. The stack of germination papers was saturated with deionized water every day and seeds were kept open to atmosphere for few minutes daily. Corn roots of length 4-5cm were placed within the rhizobox on the surface of wet paper stack. The whole experiment was carried out in dark.

3. CHARACTERIZATION SET UP

3.1. Rhizobox for hydrotropic study

The layout and cross sectional view of the hydrotropic study platform constructed for tropic response of plant roots (corn seedlings) is as shown in figure below (figure 1).

This study platform was fabricated using one glass plate and one acryl sheet (15x10 cm) separated by two layers of rubber spacer (Ethylene propylene diene monomer (EPDM) Mid-west rubber sales, Inc.). The top rubber spacer (around 1mm thick) was modified in such a way that it acts as both guiding structure for plant roots. The bottom rubber spacer (around 2mm thick) was modified to include a stack of filter papers (Whatmann grade 4) which acts as water supplying medium to avoid drying of plant roots and also includes channels for humid and dry gas purging (both the channels at an angle of 45 degrees to have symmetry on both sides) as shown in figure 1. Both the rubber spacers were glued onto the glass plate and acryl sheet using epoxy glue (Devcon 5minute epoxy gel). The bottom rubber spacer when glued to the acryl sheet forms required areas for wet paper stack and channels for 100%RH and 50%RH gas purging. The channel of wet paper stack was filled with layers of filter paper (Whatmann grade 4) with a top filter paper layer glued to the rubber spacer all over with the channel at an angle of approximately 45 degrees which acts as a hydrostimulant. Holes were drilled on the acryl sheet which coincides with the humid and dry channel and acts as inlet and outlet ports. Finally both the glass plate and the acryl sheet with rubber sheets attached were assembled together using silicone glue (GE 100% silicone sealant) to form the hydrotropic study platform. The assembled system was connected to 50%RH port for dry gas and 100%RH port for humid gas circulation through the filter paper. The corn roots were introduced into the system through the gaps in the rubber spacer where humidity gradient was formed because of the hydrostimulant at an angle of 45 degrees.

The assembled system has three inlet ports for 100%RH gas and one inlet port for 50%RH gas to include a set of control experiment where the root was exposed to

complete 100%RH gas and a set of gradient experiment where the root was exposed to a

quantitative humidity gradient (100/50%RH). The control experiment set up was also

introduced within the same system for simultaneous tropic analysis of corn roots.

Different humid gas mixtures (50%-100% RH) with a flow rate of 50SCCM were formed

using mass flow controllers connected to a 4-channel readout (MKS 247C, Laminar

technologies). All the gases were bubbled through bottled water for humidification before

being purged into the system. For gradient formation within the channel, both humidified

100% RH and 50%RH (i.e. dry gas) gases were flushed into the system through the gas

inlet ports. Humid 100% RH gas was purged through both the inlets to create a control

and uniform environment. Corn roots were introduced into the system through the gaps in

the rubber spacer and wrapped using a saran wrap to avoid any contact with atmospheric

humidity. Both gradient (100-50%RH) and control experiment (100-100%RH) analysis

were conducted simultaneously. The wet stack of filter papers was saturated with

deionized water before the root was introduced into the system. The growth and curvature

of the corn root within the system was analyzed from the pictures taken at specific times.

Each experiment was replicated four times to avoid any statistical errors.
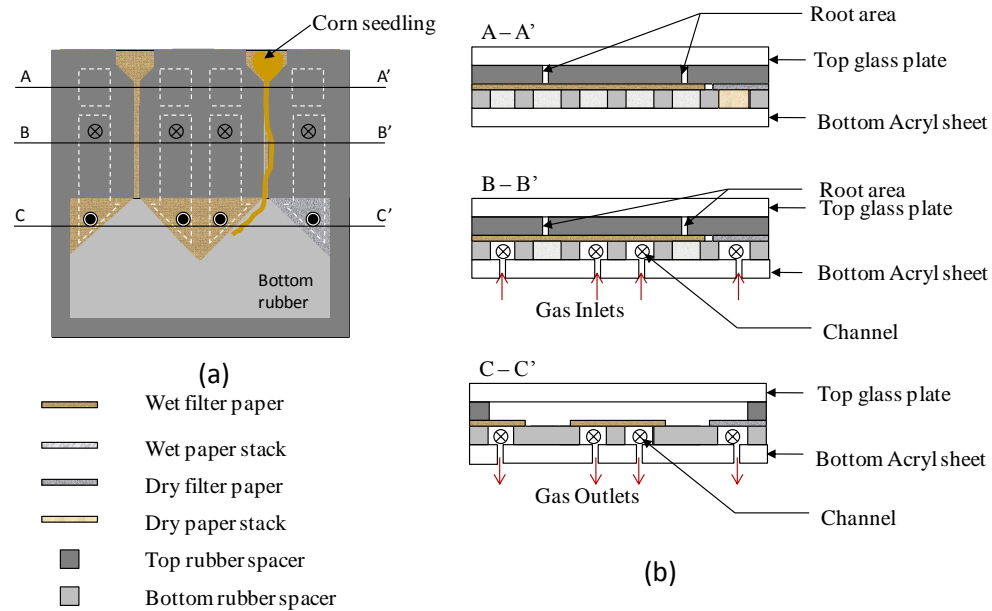
Figure 1. Hydrotropic study platform (a) Layout of the whole set up (b) cross-sectional view of the set up

3.2. Rhizobox for humidity profiling

The layout and cross sectional view of the humidity gradient study platform is as shown in figure 2. This study platform was fabricated the same way as mentioned in section 3.1 except for the custom-made humidity sheet (AGM container controls Inc.), with the ideal sensing range of 80-90%RH, embedded within the set up. Unlike hydrotropic study platform, in this set up, the modified bottom rubber sheet along with bottom glass plate was attached to the modified top rubber sheet without any attached top glass plate. And then a thin dialysis membrane along with the custom made humidity sheet was attached to the top glass plate using double-sided tape. And finally the top glass plate was attached to the integrated rubber sheets using double-sided tape as shown in figure 2.
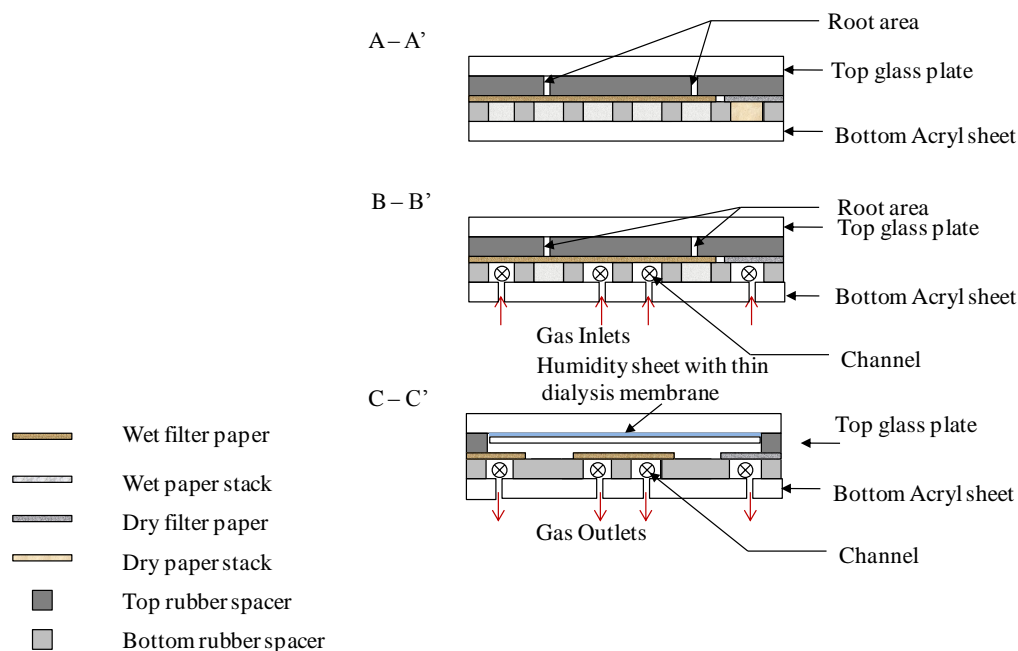
Figure 2. Study platform for humidity profiling (cross-sectional view A-A', B-B', C-C' as in figure 1)

As mentioned in the above section, different humid gases (100-50%RH) were purged through the gas inlets with a flow rate of 50SCCM for humidity gradient analysis. Images were taken at different time intervals up to 48hrs and analyzed using imageJ.

4. RESULTS AND DISCUSSION

4.1. Humidity gradient characterization

Humidity distribution image of the sensor platform was created by using gases with different percentage of relative humidities (50% and 100% RH). As mentioned in section 3.1, a control humidity environment was created by purging 100%RH gases from both the channels and simultaneously a gradient humidity environment was created by purging 100%RH and 50%RH gases from both the channels respectively. Images were taken at regular intervals of time up to 48hrs and then red extraction analysis was carried

out on all the images using imageJ. Image taken after creating humidity gradient by purging different ratios of humid gases for 1hr is displayed in figure 3. As shown in the image, different color range from blue to pink was observed with varying humidity of 50%-100%RH. Using imageJ the color images were modified into red extracted images for humidity quantification. A specific region of interest (ROI) near the gas inlets from red extracted image of figure 3 was cropped to get the red extracted intensity values with respect to varying humidity gases from 50% to 100%RH respectively which produces the calibration curve (figure 4) for further analysis of humidity gradient. From our previous work it has been concluded that the custom-made humidity sheet has a linear sensitivity in the range of 50-100%RH. Based on the sensor linearity, a two-point calibration curve was obtained within the range of 50-100%RH for humidity quantification.
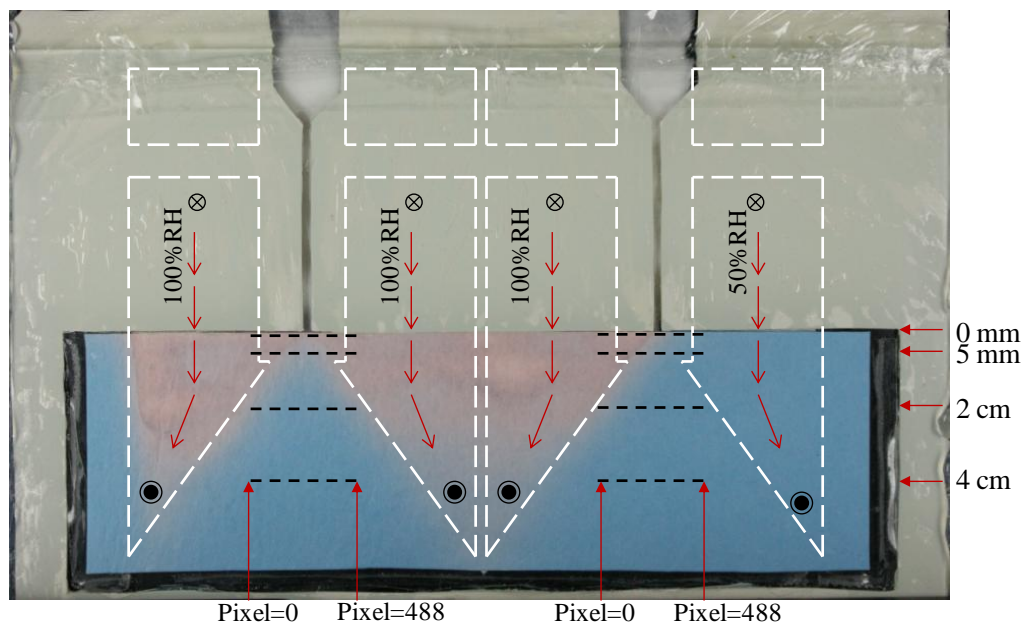
Figure 3. Humidity profile image at t=1hr with black dashed lines indicating different positions for humidity quantification and white dashed lines indicating contour of bottom channels with varying humidity gases being purged
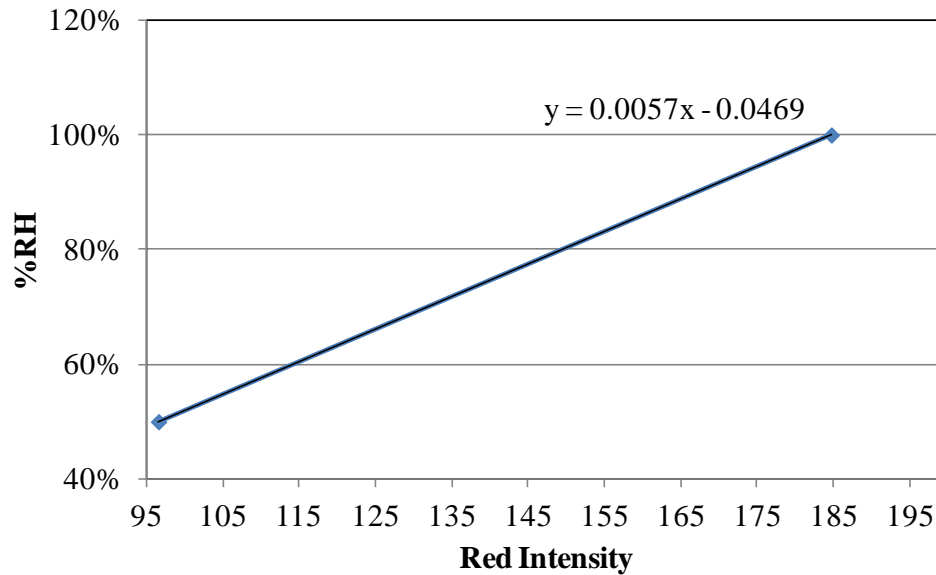
Figure 4. Calibration curve with respect to red extracted values obtained from imageJ

Using the above calibration curve, humidity gradient quantification at different positions (black dashed lines shown in figure 3) within the rhizobox has been analyzed. Humidity analysis at different time interval for both 100/100%RH and 100/50%RH gradient experiments was carried out and plotted as shown in figure 5. The humidity time profile was plotted at a particular position of 5mm within the rhizobox because of the immediate effect of humidity gradient at this position on the plant root. Figure 5(a) represents the time profile @ 100/100%RH where as figure 5(b) represents the time profile @ 100/50%RH. This represents that an effective humidity gradient has been formed @ 5mm which has a strong effect on corn roots. The spatial humidity profile has also been plotted as shown in figure 6. Different humid gases were purged within the rhizobox for a period of 24hrs for spatial analysis at different positions as marked in figure 3. From figure 6 it can be concluded that humidity gradient has been created near the vicinity of the plant root which helps in studying the hydrotropic response of small plant roots.
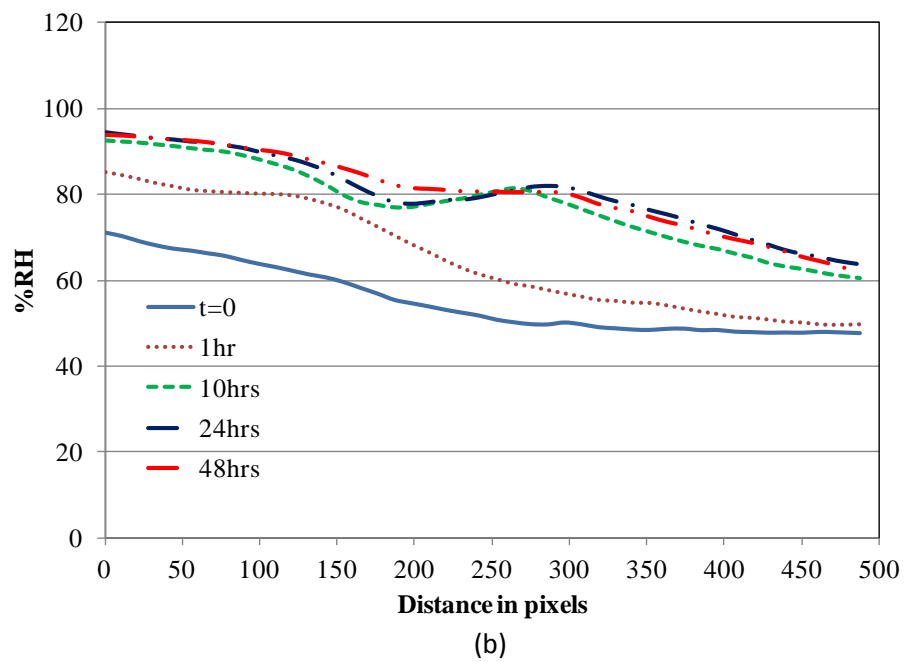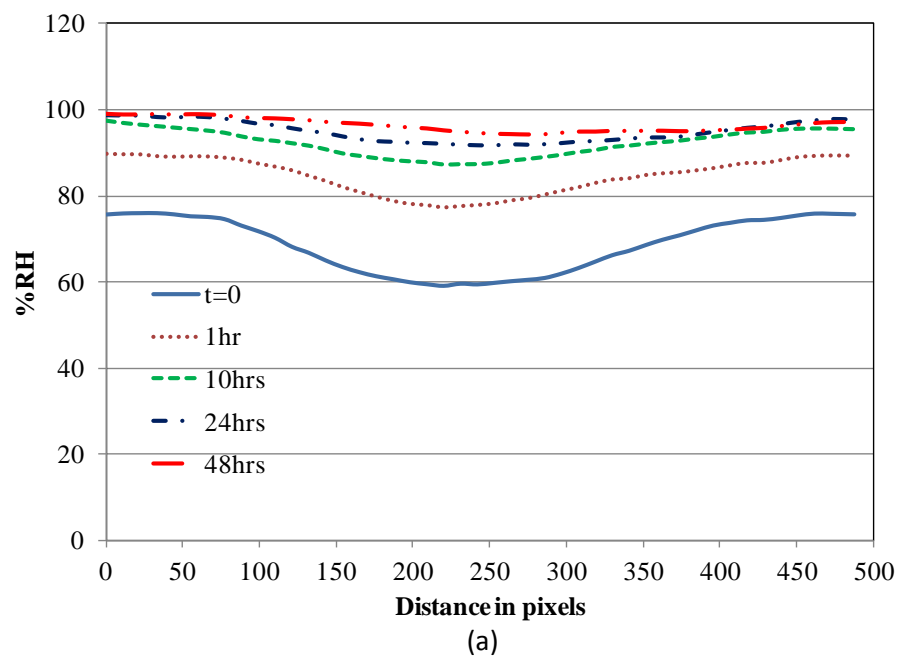
Figure 5. Time profile of humidity imaging (a) 100/100%RH @ 5mm (b) 100/50%RH @ 5mm
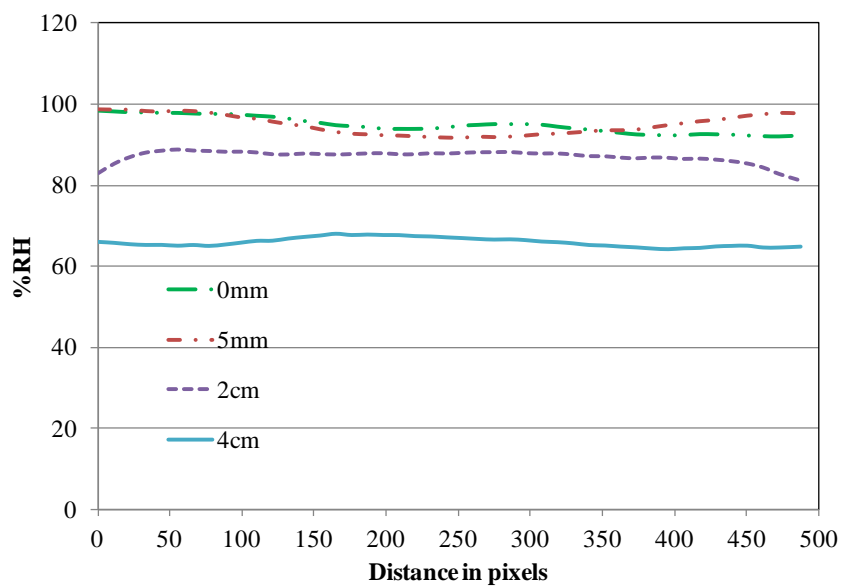
(a)
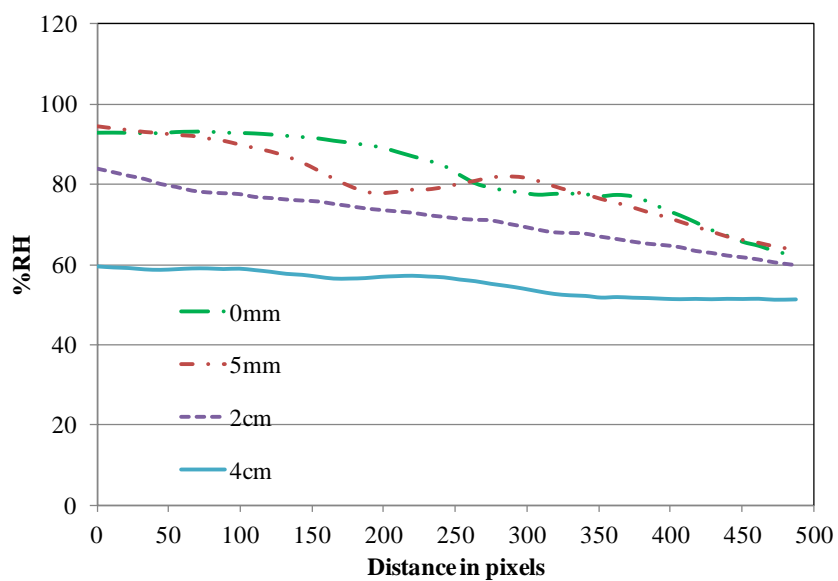
(b)

Figure 6. Humidity gradient profile at different positions within the channel after 24hrs of gas purging (a) 100%RH and 100%RH gases purged within the channel (b) 100%RH and 50%RH gases purged within the channel

4.2. Effect of humidity gradient on corn roots

Two corn kernels with same root length were placed within the rhizobox

mentioned in section 3.1 for simultaneous analysis of gradient and control experiments.

The wet filter paper stacks were saturated with deionized water before placing the corn

roots. Humidity gradient was formed within the rhizobox by purging different humid

gases for 36hrs through the inlets with a flow rate of 50SCCM as mentioned in the

previous section and with humidity profiling at different positions as shown in figure 6.

Images of the rhizobox with corn roots were taken at regular time intervals for a period of

36hrs. Figure 7 represents the timely response of the corn roots towards the

hydrostimulant with respect to the degree of humidity gradient created in the vicinity of

the root. Left side of the image represents a set of control experiment where the root is

exposed to 100%RH gas from both the sides, whereas right side of the image represents a

set of hydrotropic experiment with 100%RH from one side and 50%RH gas from the

other. All the hydrotropically oriented plant root experiments (100/50%RH) were

compared with the control experiments where the root tip is exposed to 100%RH gas

from both the sides. From figure 7 it can be clearly stated that the roots grow towards

gravity when there is no humidity gradient effect on them. All the experiments were

replicated each four times to confirm their hydrotropic response and to neglect the effect

of any errors on hydrotropic response of corn roots. Also figure 8 represents the different

degree of orientation of corn roots with respect to varying humidity gradient formed.
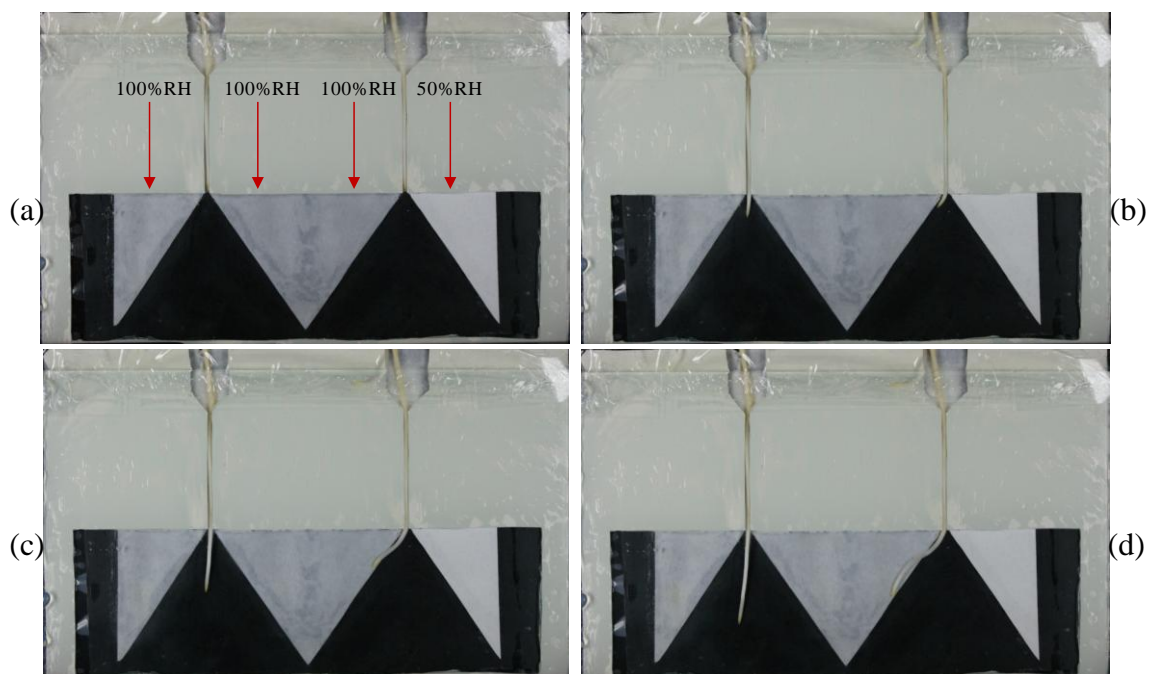
Figure 7. Time profile for control experiment and hydrotropism (100/50%RH) of corn root (a) t=0 (b) t=8hrs (c) t=16hrs (d) t=24hrs
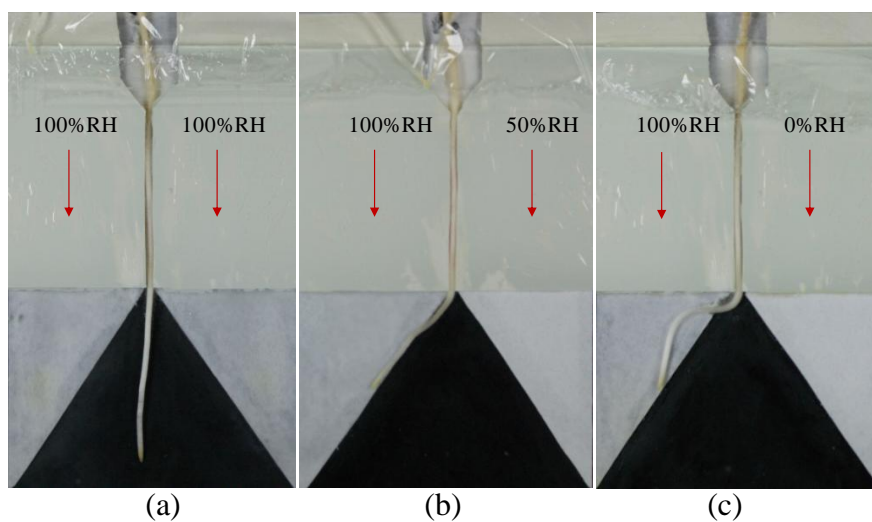
Figure 8. Root hydrotropic response @ 30hrs with respect to varying humidity (a) 100/100%RH (b) 100/50%RH (c) 100/0%RH

The effect of varying humidity gradient on plant roots has also been analyzed by purging different gases within the rhizobox. Complete dry gas (0%RH) was purged through the rhizobox to study the effect of the humidity gradient on corn roots along with gradient formed by purging 100/50%RH gases. Figure 8 represents the different degree of orientation of corn roots with respect to varying humidity gradient formed. From the above analysis it can be concluded that a very high degree of plant root orientation towards the hydrostimulant was observed with very steep humidity gradient creation within the rhizobox.

Curvature and elongation rate of the roots exposed to different conditions were measured by analyzing the images taken at regular intervals using imageJ. Curvature of roots towards and away from higher humid area was designated as +90 and -90 degrees respectively. However, different curvature kinetics was observed for different humidity atmosphere (figure 9(a)). The degree of orientation was observed to be around 40 degrees when the root was exposed to 50%RH from one side and around 55 degrees when exposed to 0%RH from one side. Whereas little curvature was observed when 100%RH gas was flushed from both the inlets. The above figures and plots confirm the hydrotropic response of corn roots with respect to different range of humid gases purged through the rhizobox. To analyze the metabolic status of plant roots, growth rate of the roots was measured for all conditions (figure 9(b)). However, the growth rate of plant roots exposed to 100/100%RH, 100/50%RH and 100/0%RH gases were statistically very different.
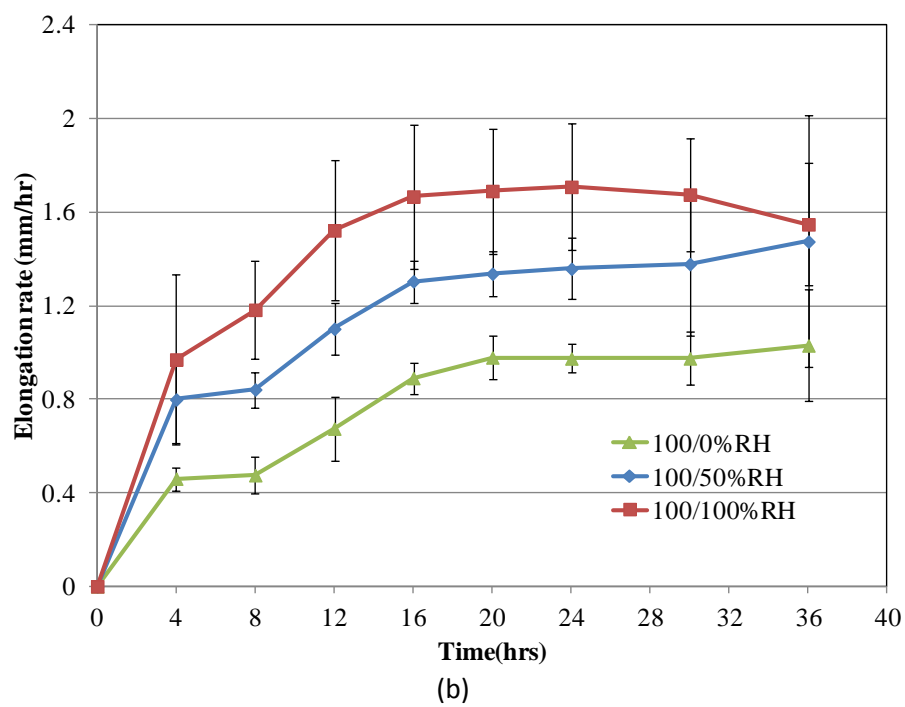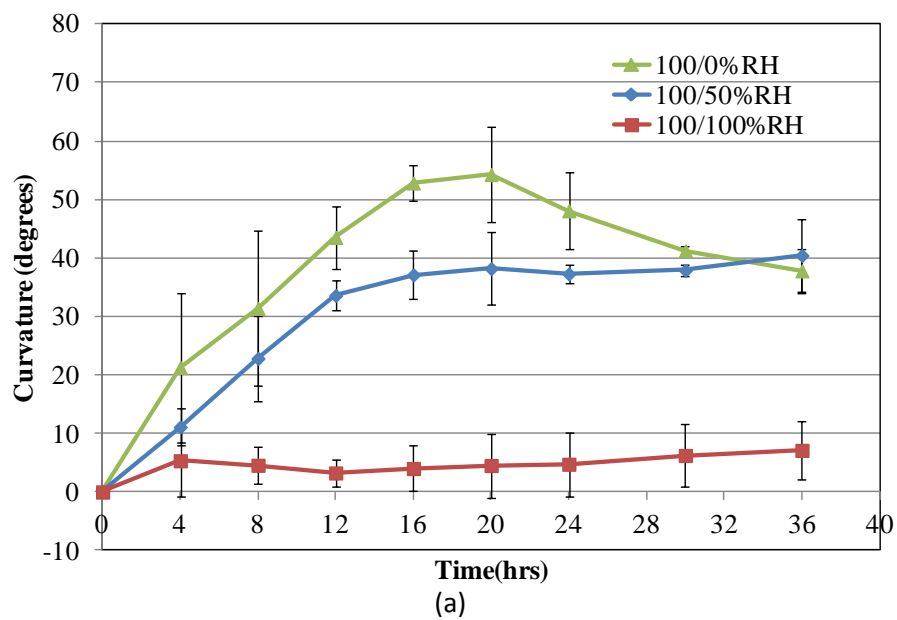
Figure 9. (a) Curvature with respect to different gradient conditions (b) Growth rate kinetics with respect to different gradient conditions (n=4, error bars=SD)

5. CONCLUSIONS AND FUTURE WORK

The two-dimensional rhizobox helped in creating humidity gradient within the device with the help of a hydrostimulant at an angle of 45 degrees. Root behavior, within these devices, with respect to hydrotropic response has been observed. The work also includes the repeatability of plant response at different humidity conditions and utilization of custom-made cobalt chloride based humidity sensor to embed within the rhizobox and analyze the humidity gradient formed. The proposed technique helps in studying the tropic responses of various small plant roots with simultaneous chemical sensing. This can be further applied to other biological applications like nodule study of different legumes, etc.

REFERENCES

[1]   Yoav Waisel, Amram Eshel, "Environmental sensing and directional growth of plant roots", Plant roots-the hidden half, third edition, Marcel Dekker Inc., 2002

[2]   Hideyuki Takahashi, "Hydrotropism and its interaction with gravitropism in roots", Plant and Soil, 165, 301-308, 1994

[3]   Hideyuki Takahashi, T.K.Scott, "Intensity of hyrdostimulation for the induction of root hydrotropism and its sensing by the root cap", Plant , Cell and Environment, 16, 99-103, 1993

[4]   Hideyuki Takahashi, Hiroshi Suge, "Root hydrotropism of an agravitropic pea mutant, ageotropum", Physiological Plantarum, 82, 24-31, 1990

[5]   Hideyuki Takahashi, Tom K.Scott, "Hydrotropism and its interaction with gravitropism in maize roots", Plant Physiology, 96, 558-564, 1991

[6]   Defeena Eapen, Maria L. Barroso, "Hydrotropism: root growth responses to water", Trends in plant sciences, 10, 44-50, 2005

[7]   Defeena Eapen, Maria L. Barroso, "A no hydrotropic response root mutant that responds positively to gravitropism in Arabidopsis", Plant physiology, 131, 536-546, 2003

[8] Nobuyuki Takahashi, Nobuharu Goto, "Hydrotropism in abscisic acid, wavy, and gravitropic mutants of Arabidopsis thaliana", Planta, 216, 203-211, 2002

[9] Hideyuki Takahashi, "Hydrotropism: the current state of our knowledge", Journal of plant research, 110, 163-169, 1997

[10] Charles Stinemetx, Hideyuki Takahashi, "Characterization of hydrotropism: the timing of perception and signal movement from the root cap in the agravitropic pea mutant Ageotropum", Plant cell physiology, 36, 800-805, 1996

[11] T.L.Yeo, T.Sun, "Fiber-optic sensor technologies for humidity and moisture measurement",   Sensors and Actuators A, 144, 280-295, 2008

[12] Z.M.Rittersma, "Recent achievements in miniaturized humidity sensors-a review of transduction techniques", Sensors and Actuators A, 96, 196-210, 2002

[13] Zhi Chen, Chi Lu, "Humidity sensors: A review of materials and mechanisms", Sensor Letters, 3, 274-295, 2005

[14] Chia-Yen Lee, Gwo-Bin Lee, "Humidity sensors: A review", Sensor Letters, 3, 1-15, 2005

[15] Candido Bariain, Ignacio R.Matias, "Optical fiber humidity sensor based on a tapered fiber coated with agarose gel", Sensors and Actuators B, 69, 127-131, 2000

[16] Jesus M.Corres, Francisco J.Arregui, "Sensitivity and optimization of tapered optical fiber humidity sensors by means of tuning the thickness of nanostructured sensitive coatings", Sensors and Actuators B, 122, 442-449, 2007

[17] Shinzo Muto, Akihiko Fukasawa, "Optical detection of moisture in air and in soil using dye doped plasti fibers", Japanese Journal of Applied Physics, 29, 1023-1025, 1990

[18] Francisco J.Arregui, Zuri Ciaurriz, "An experimental study about hydrogels for the fabrication of optical fiber humidity sensors", Sensors and Actuators B, 96, 165-172, 2003

[19] Francisca Boltinghouse, Kenneth Abel, "Development of an optical relative humidity sensor. cobalt chloride optical absorbency sensor study", Analytical Chemistry, 61, 1863-1866, 1989

[20] Sunil K.Khijwania, Kirthi K.Srinivasan, "Performance optimized optical fiber sensor for humidity measurement", Optical Engineering, 44, 2005

[21] C.M.Tay, k..Tan, "Humidity sensing using plastic optical fibers", Microwave And Optical Technology Letters", 43, 387-390, 2004

[22] Pabitra Nath, Hidam Kumarjit Singh, "Cobalt chloride doped polymer film for relative humidity measurement", Sensors and Transducers, 91, 127-133, 2008

[23] M.E.Solomon, "The use of cobalt salts as indicators of humidity and moisture", Annals Of Applied Biology, 32, 75-85, 1945

IV. FLUIDIC DEVICE TO STUDY HYDROTROPISM OF
SMALL PLANT ROOTS

ABSTRACT

Studying plant root responses to various environmental stimuli is challenging because of the controlled environmental conditions required for analysis. The other challenge includes simultaneous and effective way of environmental condition analysis with respect to plant root behavior. We report a simple fluidic device to create controlled environmental conditions to induce tropic responses along with embedded humidity sensors for simultaneous analysis of the environment surrounding the root. The Y-junction fluidic channel of the device was used for creating humidity gradient within the device to study hydrotropic response of plant roots. Different humid gases were purged though the fluidic device in such a way that a flow was created for effective humidity gradient formation. Plant roots were directly exposed to different intensity of humidity gradient and root kinetics was analyzed respectively. Successfully created and analyzed the humidity gradient which resulted in root orientation because of hydrotropic response indicating the effectiveness of this device for further biological applications.

Keywords

Environmental stimuli, Humidity gradient, Hydrotropic response

1. INTRODUCTION

Plant roots are sensitive to different kinds of tropic responses for their survival. They can easily change their growth direction with respect to elongation when they sense any favorable conditions nearby. This helps them in risky and drought conditions. The different environmental stimuli include gravitropism, hydrotropism, oxytropism and thigmotropism important for the survival of terrestrial plants. All these stimuli, other than gravitropism, are not well explored or analyzed [1].

Many lab-on-a-chip fluidic platforms have been fabricated which can mimic microenvironment gradients for cell culture systems. Most of the work was focused on polymer based micro fluidics for various analyses such as oxygen sensing, pH sensing, etc. Other than the chemical analysis, work has also been done to mimic environment gradient within cancer cells by Colin et al. group which helped in analyzing the behavior of cancer cells and the effect of the drugs on these cells. Polymer layer was used as spacer for the fluid flow. Another representative work includes fabrication of a three-chamber microscale cell culture system for toxological and pharmalogical testing. As safety plays very important role in each and every industry, it is necessary to test chemicals before use. Their work was focused on fabricating a cell culture such that toxicology profiles of different chemicals on cell culture can be analyzed easily [2-7].

From this development, focus was shifted towards plant tropic analysis using these microfluidic devices. PDMS was again used as the fluidic chip material because of its optical transparency and easy visualization of plant roots. The work done by Meier et al. was focused on chemical stimulation of Arabidopsis root with an auxin derivative along with fluorescence visualization of fluid flow. Later work included time-resolved

growth monitoring of plant root with the help of an integrated microfluidic chip. It helps in analyzing root biology with imaging at subcellular level [8-10].

With this background information, we focused on creating a meso-scale Y-junction fluidic device for studying the hydrotropic behavior on plant roots with integrated chemical sensors within the device. Custom-made humidity sensors were used for colorimetric analysis of humidity in the range of 50-100%RH. These integrated sensors help in quantitative analysis of the gradients being formed using the fluidic channels with simultaneous observation of plant behavior. Laminar flow was maintained to create effective humidity gradient. Red extraction analysis of color images using imageJ gives excellent interpretation of humidity values with respect to extracted red intensity values. A charge-coupled device (CCD) camera was used for both chemical sensing and structural imaging of the plant root.

2. GERMINATION PROTOCOL

8 to 10 corn seeds (variety B73) were placed on stack of germination papers saturated with deionized water inside a petri dish. The whole set up was wrapped with a porous tape for air exchange. The petri dish was placed vertically in dark for 4-5 days until roots of length 4-5cm were formed. The stack of germination papers were saturated with deionized water every day and seeds were kept open to atmosphere for few minutes daily. Corn roots of length 4-5cm were placed within the rhizobox on the surface of wet paper stack. The whole experiment was carried out in dark.

3. CHARACTERIZATION SET UP

3.1. Y-junction fluidic device for hydrotropic study

The layout and cross sectional view of the hydrotropic study platform constructed for tropic response of plant roots (corn seedlings) is as shown in figure below (figure 1). This study platform was fabricated using two glass plates (15x10 cm) separated by two layers of rubber spacer (Ethylene propylene diene monomer (EPDM) Mid-west rubber sales, Inc.). The top rubber spacer (around 1mm thick) cut in the Y-shape acts as both guiding structure for plant roots and also as a channel for gas flow. The bottom rubber spacer (around 2mm thick) was modified to include a stack of filter papers (Whatmann grade 4) which acts as water supplying medium to avoid drying of plant roots. Both the rubber spacers were glued onto the glass plates using epoxy glue (Devcon 5minute epoxy gel). Finally both the glass plates with modified rubber sheets on each of the glass plates were assembled together using silicone glue (GE 100% silicone sealant) to form the hydrotropic study platform. The assembled system includes two y-junction channels with wet paper stack and with two gas inlets for each channel. One y-junction channel is used for humidity gradient analysis by purging different humid gases through the channel whereas other channel is used for control experiment analysis by flushing 100%RH gas through the channel. The control experiment set up was also introduced within the same system for simultaneous tropic analysis of corn roots. Different humid gas mixtures (25%-100% RH) with a flow rate of 50SCCM were formed using mass flow controllers connected to a 4-channel readout (MKS 247C, Laminar technologies). All the gases were bubbled through bottled water for humidification before being purged into the system. For gradient formation within the channel, both humidified 100% RH and 25% or 50% or

75%RH (i.e. dry gas) gases were flushed into the system through the gas inlet ports. Humid 100% RH gas was purged through both the inlets to create a control and uniform environment. Corn roots were introduced into the system through the gaps in the rubber spacer and wrapped using a saran wrap to avoid any contact with atmospheric humidity. Both gradient (100-25%RH, 100-50%RH, and 100-75% RH) and control experiment (100-100%RH) analysis were conducted simultaneously. The wet stack of filter papers was saturated with deionized water before the root was introduced into the system. The growth and curvature of the corn root within the system was analyzed from the pictures taken at specific times. Each experiment was replicated four times to avoid any statistical errors.
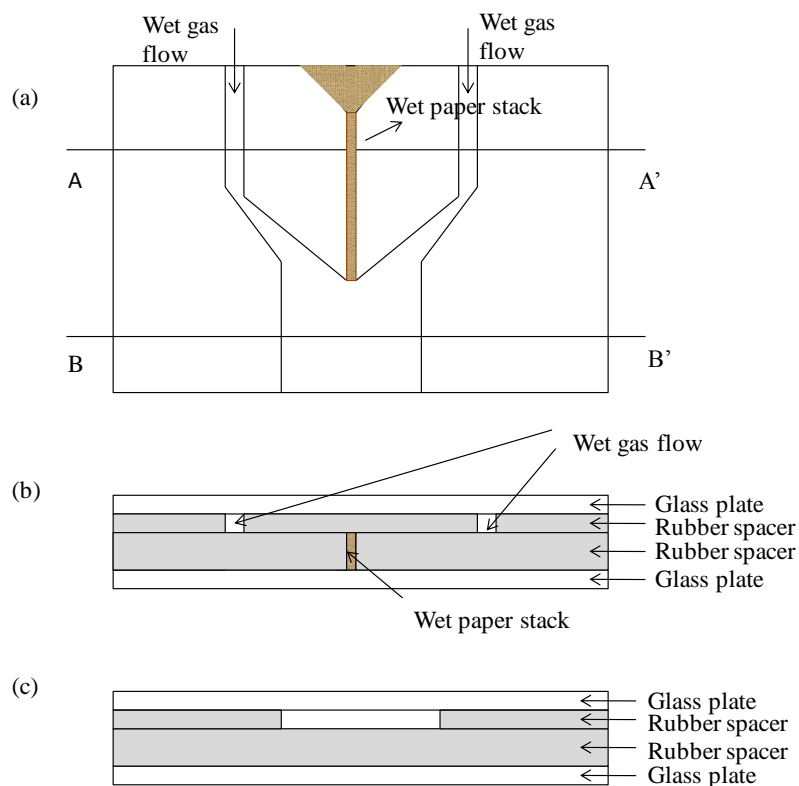
Figure 1. Hydrotropic study platform (a) Layout (b) Cross-sectional view of (A-A') (c) Cross-sectional view of (B-B')

3.2. Y-junction fluidic device for humidity profiling

The layout and cross sectional view of the humidity gradient study platform is as shown in figure 2. This study platform was fabricated the same way as mentioned in section 4.3.1 except for the custom-made humidity sheet (AGM container controls Inc.) with the ideal sensing range of 80-90%RH within the set up. Unlike hydrotropic study platform, in this set up, the modified bottom rubber sheet along with bottom glass plate was attached to the modified top rubber sheet without any attached top glass plate. And then a thin dialysis membrane along with the custom made humidity sheet was attached to the top glass plate using double-sided tape. And finally the top glass plate was attached to the integrated rubber sheets using double-sided tape as shown in figure 2.
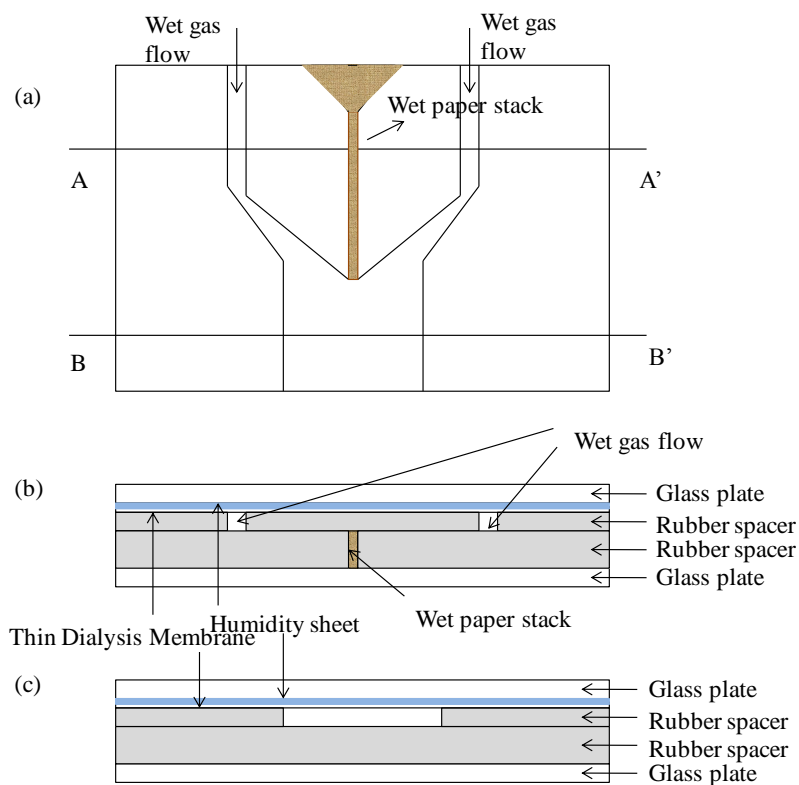
Figure 2. Layout and cross-sectional view of study platform for humidity profiling

As mentioned in the above section, different humid gases (100-25%RH, 100-50%RH, and 100-75% RH) were purged through the gas inlets with a flow rate of 50SCCM for humidity gradient analysis. Images were taken at different time intervals up to 24hrs and analyzed using imageJ.

4. RESULTS AND DISCUSSION

4.1. Humidity gradient characterization

Humidity distribution image of the y-junction sensor platform was created by using gases with different percentage of relative humidities (25%, 50%, 75% and 100% RH). Images were taken at regular intervals of time up to 24hrs and then red extraction analysis was carried out on all the images using imageJ. An image taken after 2hrs of gas purging is shown in figure 3.
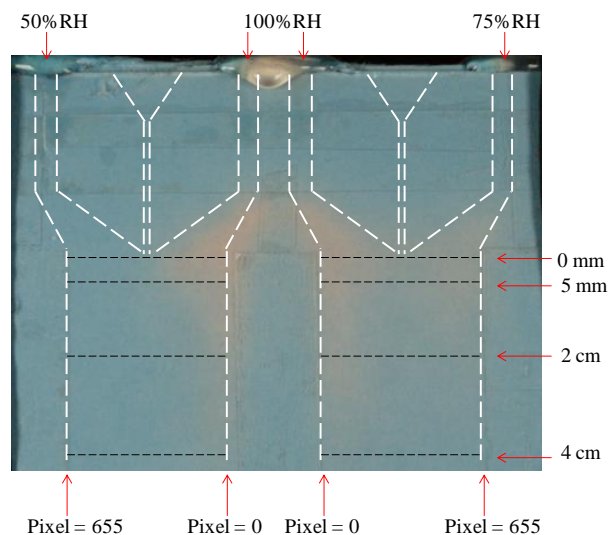
Figure 3. Humidity profile image at 2hrs with black dashed lines indicating different positions for humidity quantification and white dashed lines indicating contour of bottom channels with varying humidity gases being purged

The image taken after creating humidity gradient by purging different ratios of humid gases for 2hrs was displayed in figure 3. As shown in the image, different color range from blue to pink was observed for varying humidity of 50%-100%RH. Using imageJ the color images were modified into red extracted images for humidity quantification. A specific region of interest (ROI) near the gas inlets from red extracted image of figure 3 was cropped to get the red extracted intensity values with respect to 50%, 75% and 100%RH humid gases respectively which produces the calibration curve (figure 4) for further analysis of humidity gradient. A linear calibration curve is obtained within the range of 50-100%RH.

$$y = 0.6712x - 23.402$$
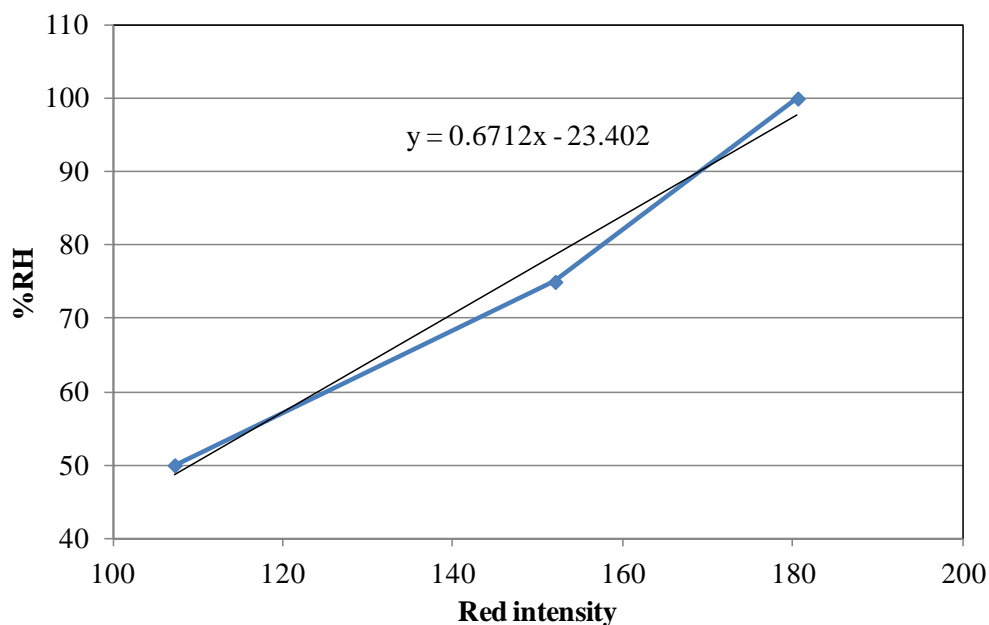
Figure 4. Calibration curve of the humidity sensor

The custom-made humidity sheet from AGM which was used for analysis ideally has a sensing range of 80-90%RH. But the practical sensing range of the humidity sheet

goes from 50%RH-100%RH as shown in the calibration curve (figure 4). Using the above calibration curve, humidity gradient quantification at different positions (black dashed lines shown in figure 3) within the fluidic device has been analyzed. Humidity analysis at different time interval for both 100/75%RH and 100/50%RH gradient experiments was carried out and plotted as shown in figure 5. The humidity time profile was plotted at a particular position of 5mm within the fluidic device because of the immediate effect of humidity gradient at this position on the plant root. Figure 5(a) represents the time profile @ 100/50%RH where as figure 5(b) represents the time profile @ 100/75%RH. This represents that an effective humidity gradient has been formed @ 5mm which has a strong effect on corn roots. The spatial humidity profile has also been plotted as shown in figure 6. Different humid gases were purged within the fluidic device for a period of 24hrs for spatial analysis at different positions as marked in figure 3. From figure 6 it can be concluded that humidity gradient has been created near the vicinity of the plant root which helps in studying the hydrotropic response of small plant roots.

(a)

(b)
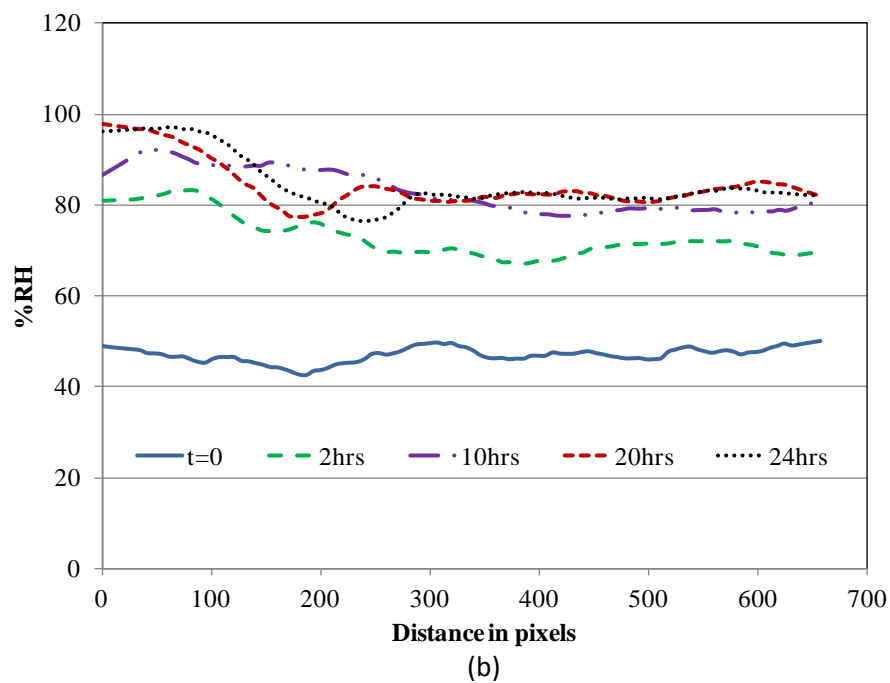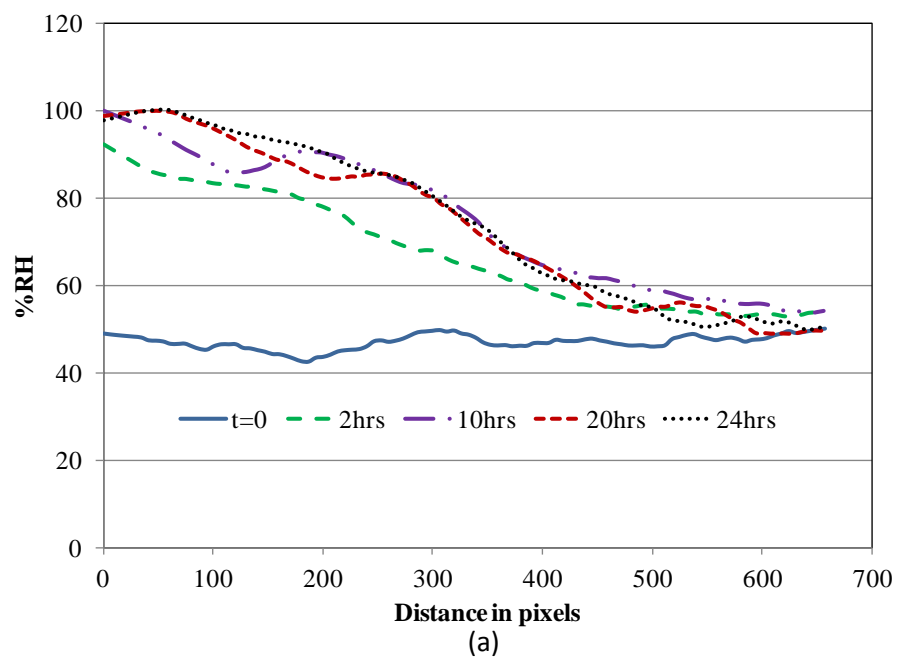
Figure 5. Time profile of humidity imaging (a) 100/50%RH @ 5mm (b) 100/75%RH @ 5mm
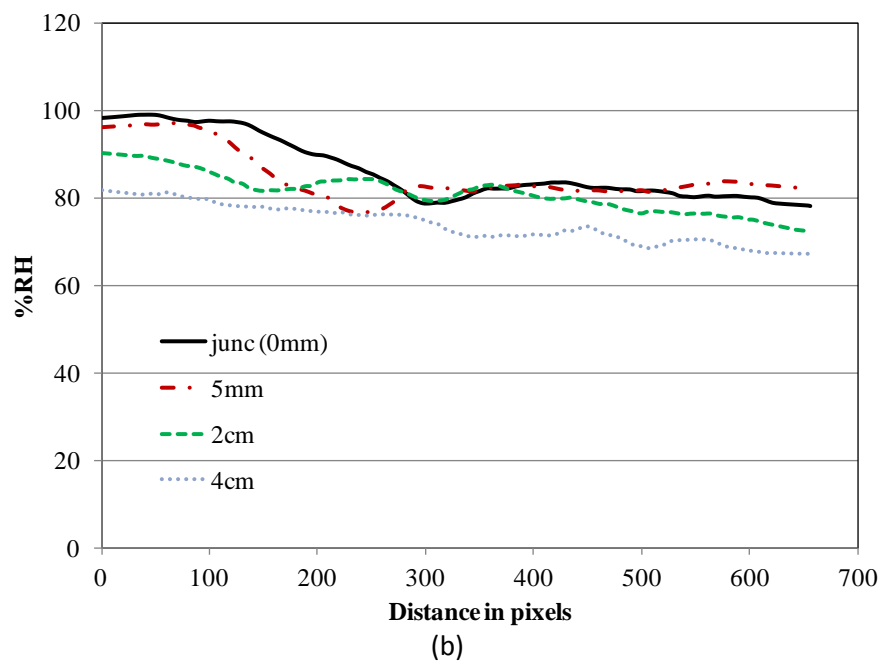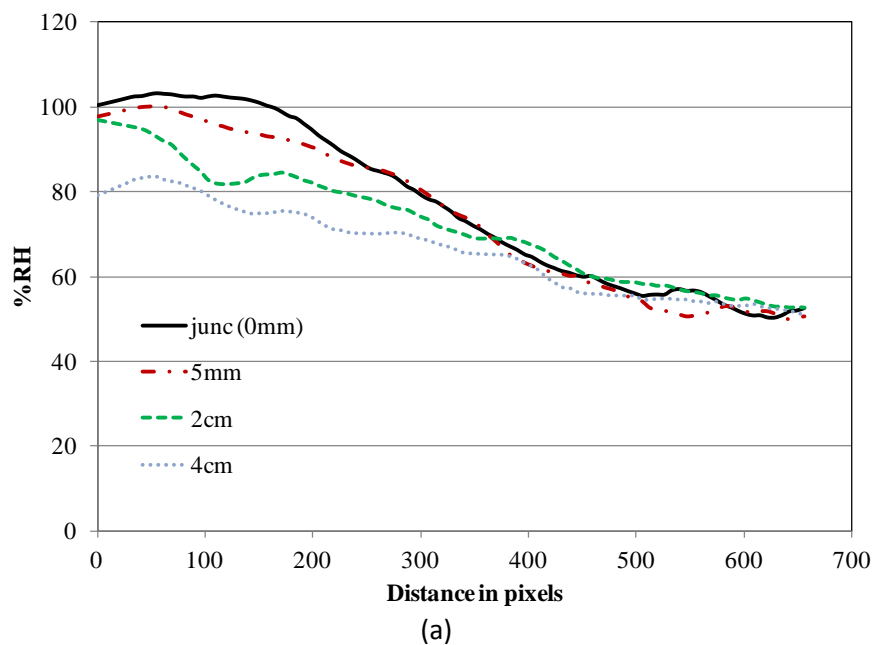
(a)

(b)

Figure 6. Humidity gradient profile at different positions within the channel after 24hrs of gas purging (a) 100%RH and 50%RH gases purged within the y-junction channel (b) 100%RH and 75%RH gases purged within the y-junction channel

4.2. Effect of humidity gradient on corn roots

Two corn kernels with same root length were placed within the rhizobox mentioned in section 3.1 for simultaneous analysis of gradient and control experiments. The wet filter paper stacks were saturated with deionized water before placing the corn roots. Humidity gradient was formed within the y-junction by purging different humid gases for 48hrs through the inlets with a flow rate of 50SCCM as mentioned in the previous section. Images were taken at regular interval of 2hrs for a period of 48hrs. From figure 7 and 8, it can be clearly stated that different hydrotropic curvatures were observed in the corn root towards the hydrostimulant depending on the degree of humidity gradient formed. All the hydrotropically oriented plant root experiments (100/25%RH, 100/50%RH, 100/75%RH) were compared with the control experiments where the root tip is exposed to 100%RH gas from both the sides. Figure 7 represents the timely response of the corn roots towards the hydrostimulant with respect to the degree of humidity gradient created in the vicinity of the root. Left side of the image represents a set of control experiment where the root is exposed to 100%RH gas from both the sides, whereas right side of the image represents a set of hydrotropic experiment with 100%RH from one side and 50%RH gas from the other. All the hydrotropically oriented plant root experiments (100/50%RH) were compared with the control experiments where the root tip is exposed to 100%RH gas from both the sides. From figure 7 and 8 it can be clearly stated that the roots grow towards gravity when there is no humidity gradient effect on them. All the experiments were replicated each four times to confirm their hydrotropic response and to neglect the effect of any errors on hydrotropic response of corn roots.

100%RH 100%RH 50%RH

(a) (b) (c) (d)

Figure 7. Time profile for control experiment and hydrotropism (100/50%RH) of corn root (a) t=0 (b) t=12hrs (c) t=24hrs (d) t=36hrs

100%RH 25%RH 100%RH 50%RH 100%RH 75%RH 100%RH 100%RH

(a) (b) (c) (d)
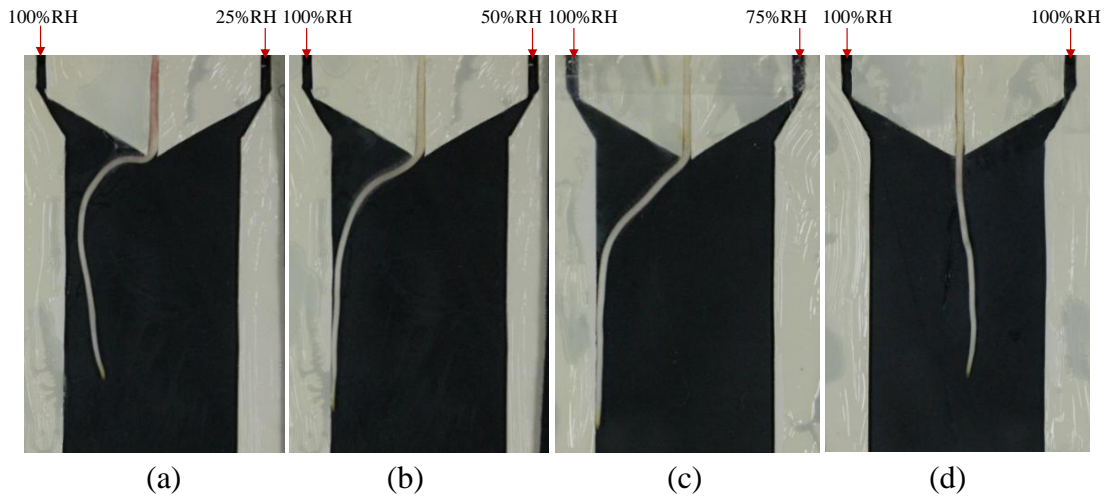
Figure 8. Effect of varying humidity gradient on corn root (a) t=48hrs, with gradient 100/25%RH (b) t=48hrs with gradient 100/50%RH (c) t=48hrs with gradient 100/75%RH (d) t=48hrs without gradient 100/100%RH

The effect of varying humidity gradient on plant roots has also been analyzed by purging different gases within the rhizobox. Figure 8 represents the different degree of orientation of corn roots with respect to varying humidity gradient formed. From the above analysis it can be concluded that a very high degree of plant root orientation towards high humid region was observed with very steep humidity gradient creation within the fluidic device.

Curvature and elongation rate of the roots exposed to different conditions were measured by analyzing the images taken at regular intervals using imageJ. Curvature of roots towards and away from higher humid area was designated as +90 and -90 degrees respectively. However, different curvature kinetics was observed for different humid atmosphere (figure 9). The degree of orientation was observed to be the highest when the root was exposed to 25%RH from one side. Whereas little curvature was observed when 100%RH gas was flushed from both the inlets. The above figures and plots confirm the hydrotropic response of corn roots with respect to different range of humid gases purged through the rhizobox. To analyze the metabolic status of plant roots, growth rate of the roots was measured for all conditions (figure 9(b)). However, the growth rate of plant roots exposed to 100/100%RH and 100/75%RH gases were not statistically different from each other. Whereas the growth rate values at 100/50%RH and 100/25%RH conditions decreased from the previous values as shown in figure 9(b).
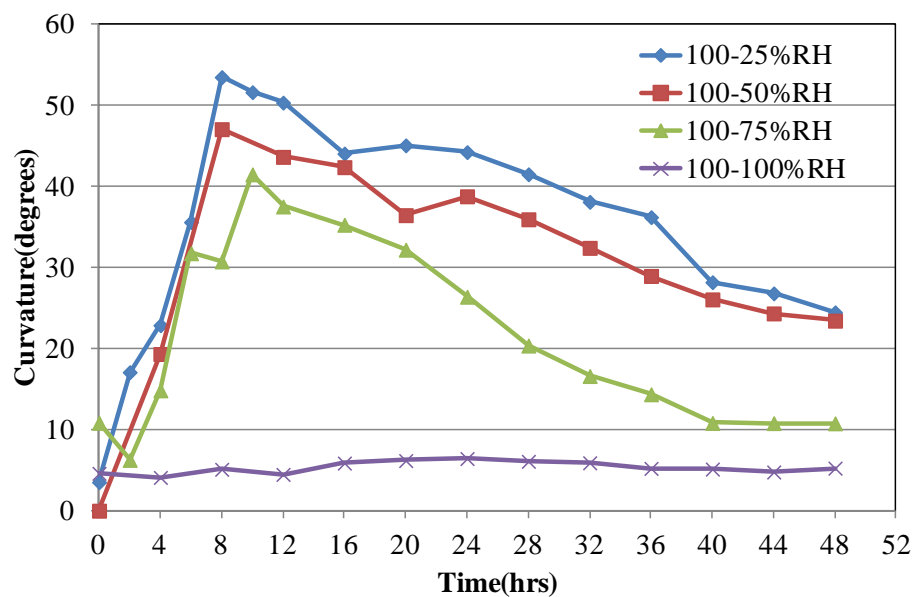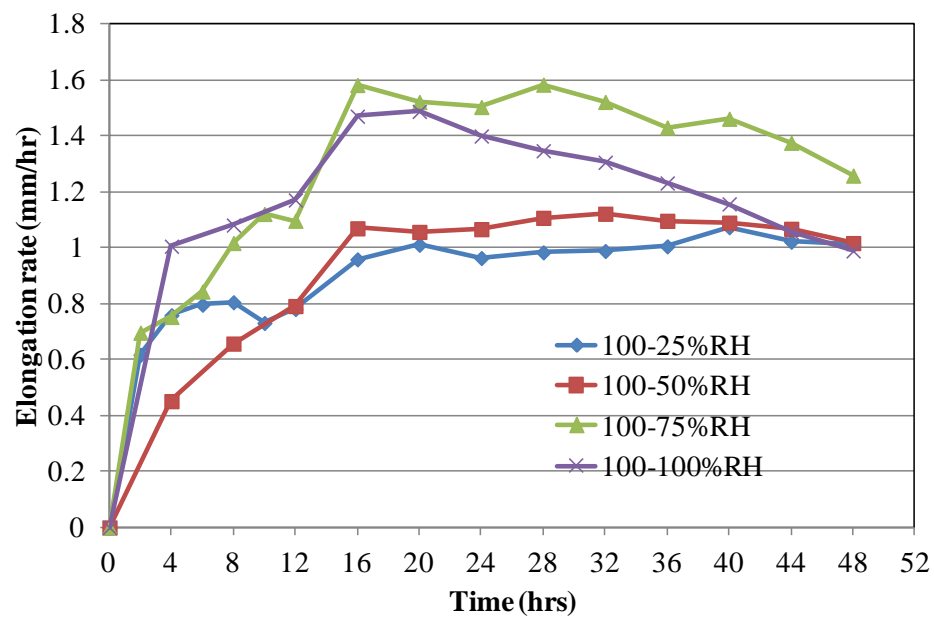
Figure 9. (a) Curvature with respect to different gradient conditions (b) Growth rate kinetics with respect to different gradient conditions (n=4)

5. CONCLUSIONS AND FUTURE WORK

The meso-scale Y-junction fluidic device helped in creating humidity gradient using laminar flow within the main channel of the Y-junction. Root behavior, within these devices, with respect to hydrotropic response has been observed. The work also includes the repeatability of plant response at different humidity conditions and utilization of custom-made cobalt chloride based humidity sensor to embed within the fluidic device and analyze the humidity gradient formed. The proposed technique helps in studying the tropic responses of various small plant roots with simultaneous chemical sensing. This can be further applied to other biological applications like nodule study of different legumes, etc.

REFERENCES

[1] Yoav Waisel, Amram Eshel, "Environmental sensing and directional growth of plant roots", Plant roots-the hidden half, third edition, Marcel Dekker Inc., 2002

[2] Aaron Sin, Katherine C. Chin, "The design and fabrication of three-chamber microscale cell culture analog devices with integrated dissolved oxygen sensors", Biotrchnology program, 20, 338-345, 2004

 [3] Svetlana M.Mirovski, Ralph G. Nuzzo, "An electrochemically driven poly(dimethylsiloxane) microfluidic actuator: oxygen sensing and programmable flows and pH gradients", Lab chip, 5, 634-645, 2005

[4]   Adam P. Vollmer, Ronald F. Probstein, "Development of an integrated microfluidic platform for dynamic oxygen sensing and delivery in a flowing medium", Lab chip, 5, 10591066, 2005

[5]   Thomas M. Keenan, Albert Folch, "Biomolecular gradients in cell culture systems", Lab on a chip, 8, 34-57, 2008

[6] Geeta Mehta, Khamir Mehta, "Quantitative measurement and control of oxygen levels in microfluidic poly(dimethylsiloxane) bioreactors during cell culture", Biomed microdevices, 9, 123-134, 2007

[7]   Colin L. Walsh, Brett M. Babin, "A multipurpose microfluidic device designed to mimic microenvironment gradients and develop targeted cancer therapeutics", Lab chip, 9, 545-554, 2009

[8]   Matthias Meier, Elena M. Lucchetta, "Chemical stimulation of the Arabidopsis thaliana root using multi-laminar flow on a microfluidic chip", Lab chip, 10, 2147-2153, 2010

[9]   Archana Parashar, Santhosh Pandey, "Plant-in-chip: Microfluidic system for studying root growth and pathogenic interactions in Arabidopsis", Applied physics letters, 98, 263703-(1-3),   2011

[10] Guido Grossman, Woei-Jiun Guo, "The rootchip: An integrated microfluidic chip for plant science", The plant cell, 23, 4234-4240, 2011

2. CONCLUSION

The above work is focused on developing oxygen and humidity sensors to embed within a meso-scale fluidic device which can be used for studying plant root response to oxytropism and hydrotropism. Optical oxygen imaging technique was utilized for two-dimensional wet oxygen analysis using a LED light panel as an excitation source and CCD camera as a photodetector. Porphyrine complex fluorophore embedded within Ethyl Cellulose (EC) matrix was used as oxygen sensitive membrane. Red extraction analysis using MATLAB was employed for oxygen quantification. Later, optical humidity sensors were developed using cobalt chloride. Humidity sensor fabrication was optimized by taking care of its sensitivity, reversibility and decreased leaching of the sensitive dye from the polymer polyvinyl alcohol (PVA). Finally, the meso-scale fluidic devices were developed to integrate these sensors within the device and successfully analyzed the gradients formed within the devices along with tropic study of small plant roots.

APPENDIX A

GERMINATION PROTOCOL

Corn

The corn species used for all the experiments are the corn B73 variety ordered from USDA seed germination department at Iowa. These seeds do not need any kind of sterilization procedure before germination. The germination papers were ordered from Anchor Paper Company. The general germination protocol of these corn seeds includes:

- 4 to 5 corn seeds were placed on stack of germination papers saturated with distilled water within a petridish

- The whole set up was wrapped with a porous tape for air exchange

- The petridish was placed vertically in dark for 4-5 days

- The stack of germination papers were saturated with distilled water every day and seeds were kept open to atmosphere for few minutes daily

- Corn roots of length 4-5cm were placed within the rhizobox on the surface of wet paper stack

- The whole experiment was carried out in dark

Alfalfa

Unlike corn seeds, alfalfa requires sterilization and dormancy break before germination. These seeds are kept inside the refrigerator @ 8°C for atleast 1-2days to break its dormancy and better germination. The sterilization and germination procedure includes:

- Alfalfa seeds were placed in 50% Clorox solution with minimum stirring for 10 minutes

- After 10 minutes, the seeds were washed with distilled water for atleast 6-7 times to remove any remains of Clorox

- In order to break dormancy of the seeds, petridish with above sterilized seeds in water was refrigerated at 8^{0}C

- After 1-2 days of dormancy breaking, seeds were placed on the surface of agarose/agar medium at room temperature

- The whole set up was wrapped with porous tape for air circulation and placed vertically under white light

- After 2-3 days of germination roots of 3-4cm length were picked and placed within the rhizobox

- Further rhizobox experiments were carried under uniform white light

Arabidopsis

Like alfalfa seeds, Arabidopsis also follows the same sterilization procedure and dormancy breaking before germination. These seeds are kept inside the refrigerator @ $8^{o}C$ for atleast 3 days to break its dormancy and better germination. The sterilization and germination procedure includes:

- Arabidopsis seeds were placed in 50% Clorox solution with minimum stirring for 10 minutes

- After 10 minutes, the seeds were washed with distilled water for atleast 6-7 times to remove any remains of Clorox

- In order to break dormancy of the seeds, petridish with above sterilized seeds in water was refrigerated at $8^{0}C$

- After 3 days of dormancy breaking, seeds were placed on the surface of agarose/agar medium at room temperature

- The whole set up was wrapped with porous tape for air circulation and placed vertically under white light

- After 2-3 days of germination roots of 3-4cm length were picked and placed within the rhizobox

APPENDIX B

DETAILED PROCEDURE OF RHIZOBOX FABRICATION

Two different devices were fabricated to study hydrotropic effect on corn roots which can be classified as Y-junction fluidic device and rhizobox with hydrostimulant.

1. Y-junction fluidic device

The fabrication procedure for Y-junction fluidic device includes:

Materials	Description
Glass plate I (top)	150x100mm size Cleaned using deionized water
Glass plate II (bottom)	Same as above
Rubber spacer I (top)	150x100mmx1mm (EPDM rubber) Modified in the shape shown in figure B.1 to include channel for gas flow and guiding structure for plant root where roots can be inserted within the fluidic device
Rubber spacer II (bottom)	150x100x2mm (EPDM rubber) Modified in the shape shown in figure B.2 to include channel of wet paper stack which helps to avoid drying of plant roots
Epoxy glue	Devcon 5minute epoxy glue for effective bonding between glass and rubber
Silicone glue	GE 100%silicone sealant for rubber to rubber bonding
Polyethylene tubing	For gas inlets
Saran wrap	To avoid contact with atm. humidity

Steps for fabrication of Y-junction fluidic device:

1. Glass plate I(top) was attached to the modified rubber spacer I (top) using epoxy glue for channel formation

2. Glass plate II (bottom) was attached to the modified rubber spacer II (bottom) using epoxy glue

3. Wet paper stack were placed in the channel formed by bottom glass plate

4. Rubber near the gas inlets/outlets was cut out to for insertion of tubings

5. Finally both the modified glass plates were attached together using silicone glue along with inlet tubings

6. Corn roots were inserted through the gaps in the rubber spacer within the fluidic device and then wrapped using saran wrap

Y-junction fluidic device fabrication

Figure. B.1 Layout of top rubber
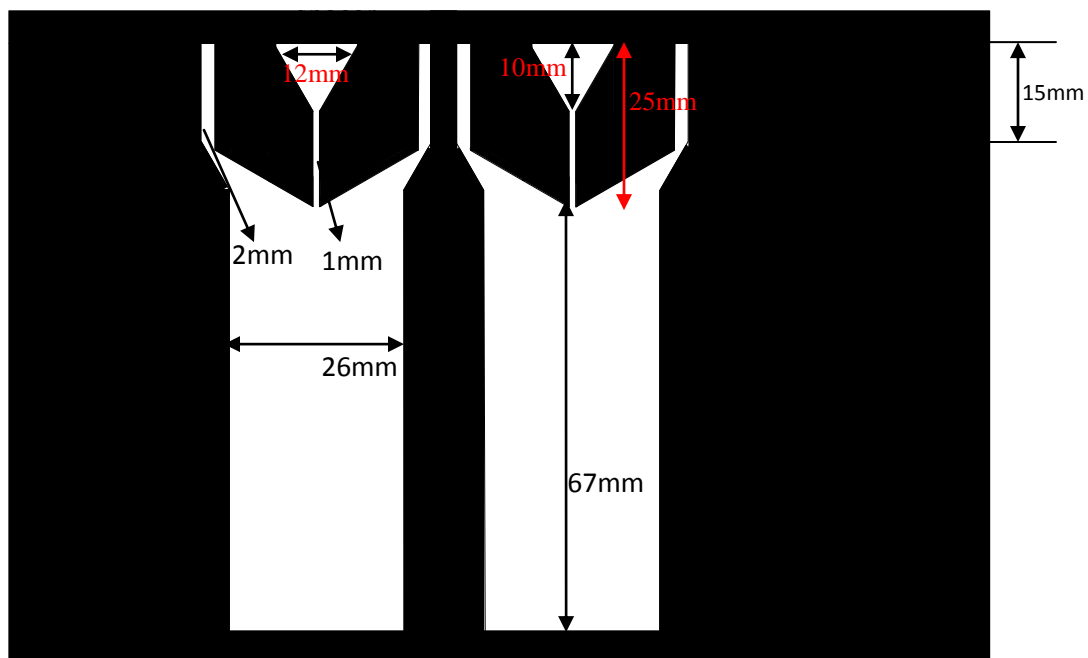
Figure. B.2 Layout of bottom rubber spacer for placing wet paper stack
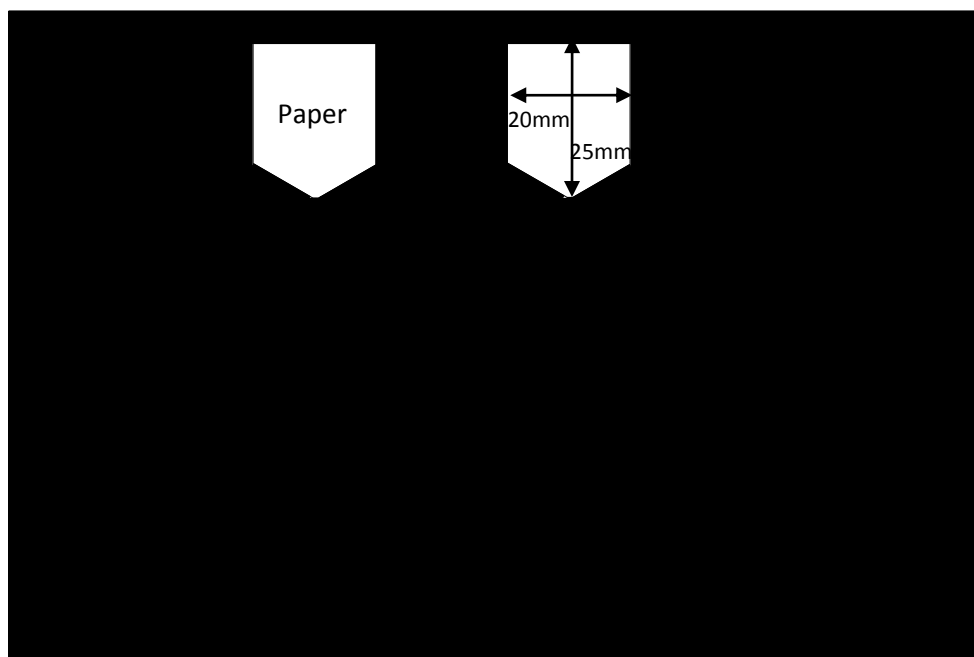
2. Rhizobox with hydrostimulant

The fabrication procedure for rhizobox with hydrostimulant is being discussed here.

Materials	Description
Glass plate (top)	150x100mm size Cleaned using deionized water
Acryl sheet (bottom)	150x100mm size Inlet and outlet holes drilled at specified positions as in figure B.3
Rubber spacer I (top)	150x100mmx1mm (EPDM rubber) Modified in the shape shown in figure B.5 guiding structure for plant root
Rubber spacer II (bottom)	150x100x2mm (EPDM rubber) Modified in the shape shown in figure B.3 to include channel of wet paper stack which helps to avoid drying of plant roots and also channels for gas purging along with the hydrostimulant
Epoxy glue	Devcon 5minute epoxy glue for effective bonding between glass and rubber
Silicone glue	GE 100%silicone sealant for rubber to rubber bonding
Polyethylene tubing	For gas inlets from back of the rhizobox
Saran wrap	To avoid contact with atm. humidity

Steps for fabrication of rhizobox with hydrostimulant:

1. Glass plate (top) was attached to the modified rubber spacer I (top) using epoxy glue to form the guiding structure for plant roots

2. Acryl sheet (bottom) with inlet and out holes was attached to the modified rubber spacer II (bottom) using epoxy glue to form channel for purging humid gases and channel for placing wet and dry paper stack

3. Wet and dry paper stack were placed in the channel formed by bottom glass plate

4. A single Whatmann filter paper (grade 4) was glued on top of the bottom rubber spacer using silicone glue and was cut in such a way that the filter paper acts as a hydrostimulant with an angle of 45 as shown in figure B.4

5. The filter paper was saturated with few drops of deionized water

6. A small slit was made on the filter paper (white dashed line) to avoid water transfer from high humid region to dry region which helps in creating humidity gradient within the rhizobox

7. Finally both the modified glass plate and acryl sheet were attached together using silicone glue along with inlet tubings attached from the back

8. Corn roots were inserted through the gaps in the rubber spacer within the rhizobox and then wrapped using saran wrap

Rhizobox with hydrostimulant

Figure. B.3 Layout of bottom rubber spacer with channels for gas purging and placing wet paper stack
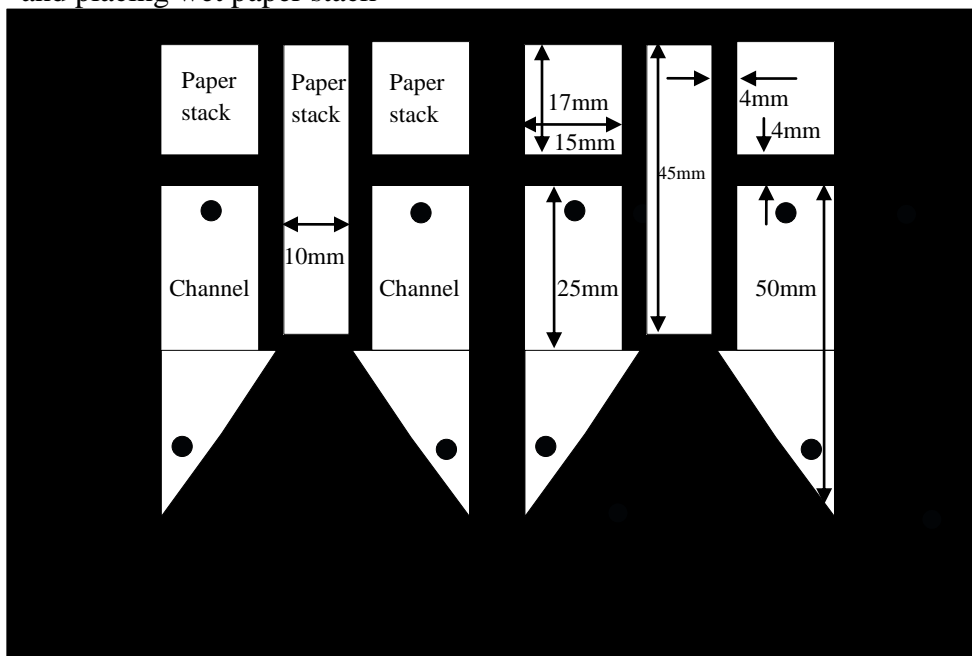
Figure. B.4 Layout of the cover filter paper layer with white dashed line for slit formation
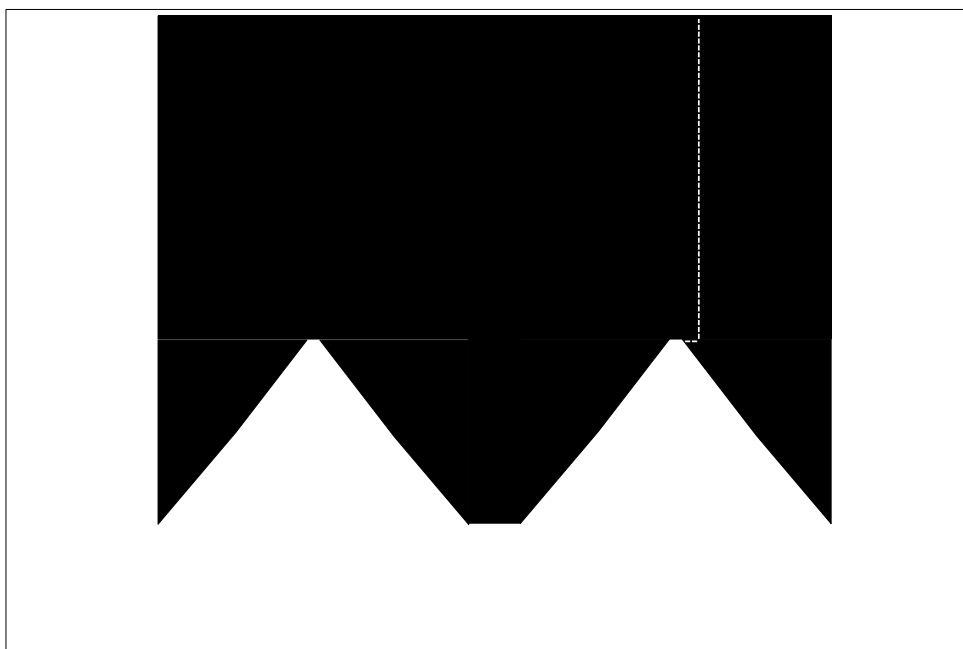
Figure. B.5 Layout of top rubber spacer as guiding structure for plant root
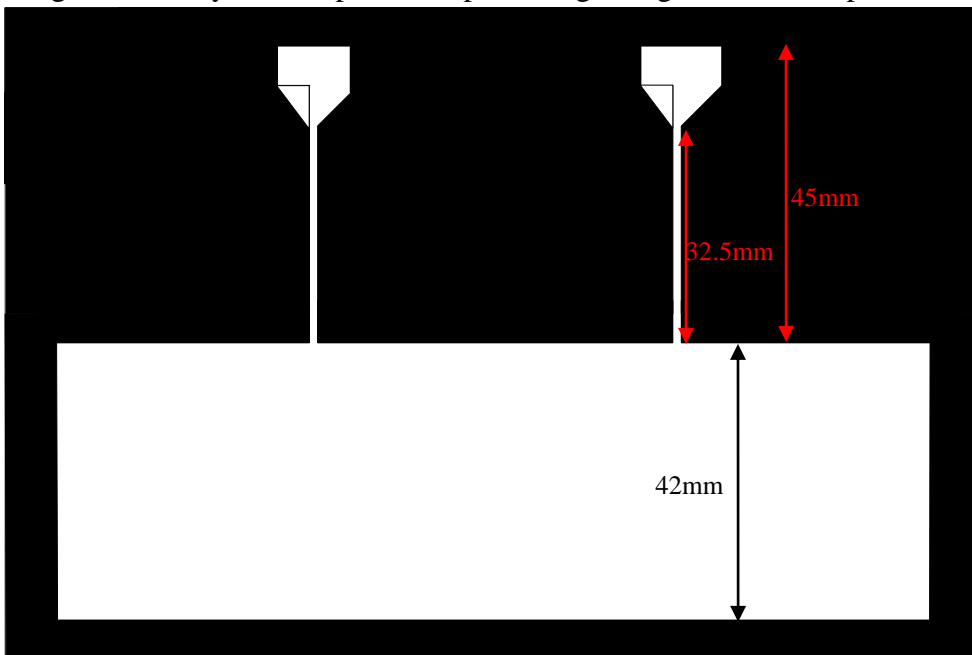
APPENDIX C

**DETAILED PROCEDURE FOR OXYGEN SENSOR COCKTAIL
PREPARATION**

Platinum porphyrine complex (PtOEP) embedded within ethyl cellulose (EC) polymer

matrix was utilized as the oxygen sensitive platform in this work of study.

Table C.1. Oxygen sensor membrane fabrication

Process	Equipment/Chemicals used	Procedure
Oxygen stock solution	Pt(II) Octaethyl porphyrine (PtOEP) from Fronteir Scientific, Tetrahydrofuran (THF)	10mg of PtOEP dissolved in 10ml of THF and stirred for 30minutes
Polymer matrix	Ethyl Cellulose (EC), Ethanol, Toluene	3g of EC dissolved in a solvent mixture of 6ml of Ethanol and 24ml of Toluene and stirred for 30minutes
Oxygen sensor cocktail	Oxygen stock solution + Polymer matrix	Both the stock solution and polymer matrix are mixed with each other and stirred
Spin coating		6ml of the cocktail was pippetted onto a glass plate and spin coated @ 300rpm for 10sec for 25microns thick sensor and placed overnight at room temperature for curing

APPENDIX D

DETAILED PROCEDURE FOR HUMIDITY SENSOR COCKTAIL PREPARATION

Cobalt chloride hexahydrate embedded within PVA matrix was employed as humidity sensitive membrane in this work. All the concentrations were optimized based on some specific properties such as leaching of the dye, stripping out of the polymer form the glass plate, response time of the membrane, etc.

Table D.1. Humidity sensor membrane fabrication

Process	Equipment/Chemicals used	Procedure
Humidity stock solution	Cobalt chloride (II) hexahydrate ($CoCl_2.6H_2O$) from Sigma-Aldrich, Water, fumed silica particles	3g of $CoCl_2.6H_2O$ dissolved in 10ml of water and stirred for 30minutes followed by mixing 0.6g of fumed silica particles into the stock solution and stirred overnight
Polymer matrix	Polyvinyl Alcohol (PVA), cross-linker Maelic acid (MA), catalyst 1M conc. H_2SO_4	1g of PVA (10wt%) dissolved in 10ml of water and heat stirred @ 80^oC for 30minutes and then 0.45g of the cross-linker (MA) along with few drops of the catalyst (1M conc. H_2SO_4) was dissolved in the PVA solution
Humidity sensor cocktail	Humidity stock solution + Polymer matrix	6ml of the stock solution was added into the polymer matrix and stirred
Spin coating		6ml of the sensor cocktail was pippetted onto a glass plate and spin coated @ 300rpm for 20sec for about 500microns thick sensor
Sandwiched humidity sensor platform	Hot plate, Thin dialysis membrane, Rubber roller	The glass plate with humidity sensing dye on it was heated

		@ 40°C for at least 6-8 minutes followed by lamination of the thin dialysis membrane on its surface with the help of the roller immediately.
Thermal esterification	Hot plate	The sandwiched humidity membrane was heated @ 80°C for 2hrs which helps in cross linking of the polymer using thermal esterification process

APPENDIX E

MATLAB CODE (m-file) FOR IMAGE PROCESSING OF THE OXYGEN SENSOR

The MATLAB m-file to produce figure 8 in paper I is as follows:

```
clear all; close all; clc

% Read original images
 %  0% Oxygen concentration
im_base=double(imread('O01.jpg'));

im_base=im_base(:,:,1);

im_add=double(imread('O02.jpg'));

im_add=im_add(:,:,1);

im_base=im_base+im_add;

im_add=double(imread('O03.jpg'));

im_add=im_add(:,:,1);

im_base=im_base+im_add;

im_add=double(imread('O04.jpg'));

im_add=im_add(:,:,1);

im_base=im_base+im_add;

im_add=double(imread('O05.jpg'));

im_add=im_add(:,:,1);

im_base=im_base+im_add;

im_add=double(imread('O06.jpg'));

im_add=im_add(:,:,1);

im_base=im_base+im_add;

im_add=double(imread('O07.jpg'));

im_add=im_add(:,:,1);

im_base=im_base+im_add;

im_add=double(imread('O08.jpg'));

im_add=im_add(:,:,1);

im_base=im_base+im_add;
```

```
im_add=double(imread('O09.jpg'));

im_add=im_add(:,:,1);

im_base=im_base+im_add;

im_add=double(imread('O010.jpg'));

im_add=im_add(:,:,1);

im_O0=im_base+im_add;

clear im_add; clear im_base; im_O0=im_O0/10;

%  5% Oxygen concentration

im_5=double(imread('O51.jpg'));

im_5=im_5(:,:,1);

im_5_add=double(imread('O52.jpg'));

im_5_add=im_5_add(:,:,1);

im_5=im_5+im_5_add;

im_5_add=double(imread('O53.jpg'));

im_5_add=im_5_add(:,:,1);

im_5=im_5+im_5_add;

im_5_add=double(imread('O54.jpg'));

im_5_add=im_5_add(:,:,1);

im_5=im_5+im_5_add;

im_5_add=double(imread('O55.jpg'));

im_5_add=im_5_add(:,:,1);

im_5=im_5+im_5_add;

im_5_add=double(imread('O56.jpg'));

im_5_add=im_5_add(:,:,1);

im_5=im_5+im_5_add;

im_5_add=double(imread('O57.jpg'));

im_5_add=im_5_add(:,:,1);

im_5=im_5+im_5_add;
```

```
im_5_add=double(imread('O58.jpg'));

im_5_add=im_5_add(:,:,1);

im_5=im_5+im_5_add;

im_5_add=double(imread('O59.jpg'));

im_5_add=im_5_add(:,:,1);

im_5=im_5+im_5_add;

im_5_add=double(imread('O510.jpg'));

im_5_add=im_5_add(:,:,1);

im_O5=im_5+im_5_add;

clear im_5_add; clear im_5; im_O5=im_O5/10;
```

% 10% Oxygen concentration

```
im_10=double(imread('O101.jpg'));

im_10=im_10(:,:,1);

im_10_add=double(imread('O102.jpg'));

im_10_add=im_10_add(:,:,1);

im_10=im_10+im_10_add;

im_10_add=double(imread('O103.jpg'));

im_10_add=im_10_add(:,:,1);

im_10=im_10+im_10_add;

im_10_add=double(imread('O104.jpg'));

im_10_add=im_10_add(:,:,1);

im_10=im_10+im_10_add;

im_10_add=double(imread('O105.jpg'));

im_10_add=im_10_add(:,:,1);

im_10=im_10+im_10_add;

im_10_add=double(imread('O106.jpg'));

im_10_add=im_10_add(:,:,1);

im_10=im_10+im_10_add;
```

```matlab
im_10_add=double(imread('O107.jpg'));

im_10_add=im_10_add(:,:,1);

im_10=im_10+im_10_add;

im_10_add=double(imread('O108.jpg'));

im_10_add=im_10_add(:,:,1);

im_10=im_10+im_10_add;

im_10_add=double(imread('O109.jpg'));

im_10_add=im_10_add(:,:,1);

im_10=im_10+im_10_add;

im_10_add=double(imread('O1010.jpg'));

im_10_add=im_10_add(:,:,1);

im_O10=im_10+im_10_add;

clear im_10_add; clear im_10; im_O10=im_O10/10;

 %  15% Oxygen

im_15=double(imread('O151.jpg'));

im_15=im_15 (:,:,1);

im_15_add=double(imread('O152.jpg'));

im_15_add=im_15_add(:,:,1);

im_15=im_15+im_15_add;

im_15_add=double(imread('O153.jpg'));

im_15_add=im_15_add(:,:,1);

im_15=im_15+im_15_add;

im_15_add=double(imread('O154.jpg'));

im_15_add=im_15_add(:,:,1);

im_15=im_15+im_15_add;

im_15_add=double(imread('O155.jpg'));

im_15_add=im_15_add(:,:,1);

im_15=im_15+im_15_add;
```

```matlab
im_15_add=double(imread('O156.jpg'));

im_15_add=im_15_add(:,:,1);

im_15=im_15+im_15_add;

im_15_add=double(imread('O157.jpg'));

im_15_add=im_15_add(:,:,1);

im_15=im_15+im_15_add;

im_15_add=double(imread('O158.jpg'));

im_15_add=im_15_add(:,:,1);

im_15=im_15+im_15_add;

im_15_add=double(imread('O159.jpg'));

im_15_add=im_15_add(:,:,1);

im_15=im_15+im_15_add;

im_15_add=double(imread('O1510.jpg'));

im_15_add=im_15_add(:,:,1);

im_O15=im_15+im_15_add;

clear im_15_add; clear im_15; im_O15=im_O15/10;

%  21% Oxygen concentration

im_21=double(imread('O211.jpg'));

im_21=im_21(:,:,1);

im_21_add=double(imread('O212.jpg'));

im_21_add=im_21_add(:,:,1);

im_21=im_21+im_21_add;

im_21_add=double(imread('O213.jpg'));

im_21_add=im_21_add(:,:,1);

im_21=im_21+im_21_add;

im_21_add=double(imread('O214.jpg'));

im_21_add=im_21_add(:,:,1);

im_21=im_21+im_21_add;
```

```
im_21_add=double(imread('O215.jpg'));

im_21_add=im_21_add(:,:,1);

im_21=im_21+im_21_add;

im_21_add=double(imread('O216.jpg'));

im_21_add=im_21_add(:,:,1);

im_21=im_21+im_21_add;

im_21_add=double(imread('O217.jpg'));

im_21_add=im_21_add(:,:,1);

im_21=im_21+im_21_add;

im_21_add=double(imread('O218.jpg'));

im_21_add=im_21_add(:,:,1);

im_21=im_21+im_21_add;

im_21_add=double(imread('O219.jpg'));

im_21_add=im_21_add(:,:,1);

im_21=im_21+im_21_add;

im_21_add=double(imread('O2110.jpg'));

im_21_add=im_21_add(:,:,1);

im_O21=im_21+im_21_add;

clear im_21_add; clear im_21; im_O21=im_O21/10;

 % ROI coordinate check

red_ex=uint8(im_O21);

imshow(red_ex); % image display

% crop point-1

mean_O0=mean(mean(imcrop(im_O0,[2746 1339 15 15])));

mean_O5=mean(mean(imcrop(im_O5,[2746 1339 15 15])));

mean_O10=mean(mean(imcrop(im_O10,[2746 1339 15 15])));

mean_O15=mean(mean(imcrop(im_O15,[2746 1339 15 15])));

mean_O21=mean(mean(imcrop(im_O21,[2746 1339 15 15])));
```

```matlab
% crop point-2

mean_O0_2=mean(mean(imcrop(im_O0,[2791 1339 15 15])));

mean_O5_2=mean(mean(imcrop(im_O5,[2791 1339 15 15])));

mean_O10_2=mean(mean(imcrop(im_O10,[2791 1339 15 15])));

mean_O15_2=mean(mean(imcrop(im_O15,[2791 1339 15 15])));

mean_O21_2=mean(mean(imcrop(im_O21,[2791 1339 15 15])));

% crop point-3

mean_O0_3=mean(mean(imcrop(im_O0,[2791 1384 15 15])));

mean_O5_3=mean(mean(imcrop(im_O5,[2791 1384 15 15])));

mean_O10_3=mean(mean(imcrop(im_O10,[2791 1384 15 15])));

mean_O15_3=mean(mean(imcrop(im_O15,[2791 1384 15 15])));

mean_O21_3=mean(mean(imcrop(im_O21,[2791 1384 15 15])));

% crop point-4

mean_O0_4=mean(mean(imcrop(im_O0,[2746 1384 15 15])));

mean_O5_4=mean(mean(imcrop(im_O5,[2746 1384 15 15])));

mean_O10_4=mean(mean(imcrop(im_O10,[2746 1384 15 15])));

mean_O15_4=mean(mean(imcrop(im_O15,[2746 1384 15 15])));

mean_O21_4=mean(mean(imcrop(im_O21,[2746 1384 15 15])));

% Average of crop areas

mean_O0_1=[mean_O0;mean_O0_2; mean_O0_3;mean_O0_4];

mean_O0=mean(mean_O0_1)

mean_O5_1=[mean_O5;mean_O5_2; mean_O5_3;mean_O5_4];

mean_O5=mean(mean_O5_1)

mean_O10_1=[mean_O10;mean_O10_2; mean_O10_3;mean_O10_4];

mean_O10=mean(mean_O10_1)

mean_O15_1=[mean_O15;mean_O15_2; mean_O15_3;mean_O15_4];

mean_O15=mean(mean_O15_1)

mean_O21_1=[mean_O21;mean_O21_2; mean_O21_3;mean_O21_4];
```

```
mean_O21=mean(mean_O21_1)
```

```
% Stern-Volmer type conversion
```

```
 SV_0=mean_O0/mean_O0;
```

```
SV_5=mean_O0/mean_O5;
```

```
SV_10=mean_O0/mean_O10;
```

```
SV_15=mean_O0/mean_O15;
```

```
SV_21=mean_O0/mean_O21;
```

```
 SV=[SV_0,SV_5,SV_10,SV_15,SV_21];
```

```
% plot result
```

```
X=[0 5 10 15 21];
```

```
Figure(200);
```

```
Plot(X SV)
```

The MATLAB m-file to produce figure 9 in paper I is as follows:

```matlab
clear all; close all; clc;
 % image read, summation, division process
% before : 0% oxygen concentration
im_base=double(imread('before1.jpg')); % change data format from uint8 to double
im_base=im_base(:,:,1); % red component extraction
im_add=double(imread('before2.jpg'));
im_add=im_add(:,:,1);
im_base=im_base+im_add; % image summation
im_add=double(imread('before3.jpg'));
im_add=im_add(:,:,1);
im_base=im_base+im_add;
im_add=double(imread('before4.jpg'));
im_add=im_add(:,:,1);
im_base=im_base+im_add;
im_add=double(imread('before5.jpg'));
im_add=im_add(:,:,1);
im_base=im_base+im_add;
im_add=double(imread('before6.jpg'));
im_add=im_add(:,:,1);
im_base=im_base+im_add;
im_add=double(imread('before7.jpg'));
im_add=im_add(:,:,1);
im_base=im_base+im_add;
im_add=double(imread('before8.jpg'));
im_add=im_add(:,:,1);
im_base=im_base+im_add;
```

```
im_add=double(imread('before9.jpg'));

im_add=im_add(:,:,1);

im_base=im_base+im_add;

im_add=double(imread('before10.jpg'));

im_add=im_add(:,:,1);

im_base=im_base+im_add;

clear im_add; im_base=im_base/10; % image division with total image number

% 30min after

im_30=double(imread('30min1.jpg'));

im_30=im_30(:,:,1);

im_30_add=double(imread('30min2.jpg'));

im_30_add=im_30_add(:,:,1);

im_30=im_30+im_30_add;

im_30_add=double(imread('30min3.jpg'));

im_30_add=im_30_add(:,:,1);

im_30=im_30+im_30_add;

im_30_add=double(imread('30min4.jpg'));

im_30_add=im_30_add(:,:,1);

im_30=im_30+im_30_add;

im_30_add=double(imread('30min5.jpg'));

im_30_add=im_30_add(:,:,1);

im_30=im_30+im_30_add;

im_30_add=double(imread('30min6.jpg'));

im_30_add=im_30_add(:,:,1);

im_30=im_30+im_30_add;

im_30_add=double(imread('30min7.jpg'));

im_30_add=im_30_add(:,:,1);

im_30=im_30+im_30_add;
```

```
im_30_add=double(imread('30min8.jpg'));

im_30_add=im_30_add(:,:,1);

im_30=im_30+im_30_add;

im_30_add=double(imread('30min9.jpg'));

im_30_add=im_30_add(:,:,1);

im_30=im_30+im_30_add;

im_30_add=double(imread('30min10.jpg'));

im_30_add=im_30_add(:,:,1);

im_30=im_30+im_30_add;

clear im_30_add; im_30=im_30/10;

 % ROI coordinate check

red_ex=uint8(im_30);

imshow(red_ex); % image display

im_base=imcrop(im_base,[1018 832 2539 1717]);

im_30=imcrop(im_10,[1018 832 2539 1717]);

% image division with 0% oxygen image for Stern-Volmer type conversion

im_base_sv=im_base./im_base;

im_30_sv=im_base./im_30;

% display entire channel 3-D image converted by Stern-Volmer type

figure(100);

mesh(im_base)

figure(200);

mesh(im_30)

figure(300);

mesh(im_30_sv)
```

APPENDIX F

IMAGE PROCESSING WITH IMAGEJ HOR HUMIDITY SENSOR

The red color extraction of oxygen sensor images was analyzed by Image J. It is freely available, Java-based image processing software developed at the National Institutes of Health (http://rsbweb.nih.gov/ij/). Table G.1 shows some of the functions of ImageJ used for the image processing.

Table G.1. Image processing procedure with ImageJ.

Menu	*Description*
File-Open	Load the image.
Edit-Selection-Specify	Set the region of interest (ROI).
Analyze-Histogram	Obtain the total color intensity (usually mean value).
Image-Color-RGB Split	Extract red color intensity.
Analyze-Plot Profile	Obtain 2-D intensity plot.
Plugins-3D-Interactive 3D Surface Plot	Obtain 3-D intensity plot.

APPENDIX G

MATLAB CODE FOR IMAGE PROCESSING OF THE HUMIDITY DISTRIBUTION WITHIN THE RHIZOBOX

Matlab code to produce figures 5 and 6 in paper III is as follows:

```matlab
clear all; close all; clc;
% input image name for analysis
% origin=imread('humidity1.jpg');
im_base=double(imread('humidity1.jpg'));
% red extraction
red=im_base(:,:,1);
% position where analysis done for the region without any gradient (0mm)
h1=1840;
% vertical positions which give end and start point for analysis
H11=red(h1,1250:1:1730);
% humidity quantification using calibration equation
V11=(0.0057*H11-.0469)*100;
% 5mm
h1=1943;
H12=red(h1,1250:1:1730);
V12=(0.0057*H12-.0469)*100;
% 2cm
h1=2216;
H13=red(h1,1250:1:1730);
V13=(0.0057*H13-.0469)*100;
% 4cm
h1=2592;
H14=red(h1,1250:1:1730);
V14=(0.0057*H14-.0469)*100;
% position where analysis done for the region with gradient (0mm)
h1=1840;
H21=red(h1,2850:1:3330);
```

```matlab
V21=(0.0057*H21-.0469)*100;

% 5mm

h1=1943;

H22=red(h1,2850:1:3330);

V22=(0.0057*H22-.0469)*100;

% 2cm

h1=2216;

H23=red(h1,2850:1:3330);

V23=(0.0057*H23-.0469)*100;

% 4cm

h1=2592;

H24=red(h1,2850:1:3330);

V24=(0.0057*H24-.0469)*100;

% plots

figure(100);

plot(V11)

figure(200);

plot(V12)

figure(300);

plot(V13)

figure(400);

plot(V14)

figure(500);

plot(V15)

figure(600);

plot(V21)

figure(700);

plot(V22)
```

```
figure(800);

plot(V23)

figure(900);

plot(V24)

figure(1000);

plot(V25)
```

VITA

Satya Gowthami Achanta was born in Hyderabad, India. In June 2007, she received her bachelor's degree in Chemical Engineering from Osmania University, Hyderabad, India where she received the prestigious gold medal for the best outgoing student in Chemical Engineering.

In August 2007, she enrolled at the Missouri University of Science and Technology-Rolla to pursue a doctoral degree in Chemical Engineering under the guidance of Dr. Chang-Soo Kim. During her time at Rolla, she was employed as a Graduate Research Assistant in the Electrical Engineering department. She received her doctoral degree from Missouri University of Science and Technology-Rolla in December 2012.